OpenNano 8 (2022) 100104

Contents lists available at ScienceDirect

OpenNano

journal homepage: www.elsevier.com/locate/onano

Metal nanoparticles-assisted early diagnosis of diseases

Maryam Jouyandeh [a], S. Mohammad Sajadi [b], Farzad Seidi [a], Sajjad Habibzadeh [c], Muhammad Tajammal Munir [d], Otman Abida [d], Sepideh Ahmadi [e], Daria Kowalkowska-Zedler [f], Navid Rabiee [g,h,*], Mohammad Rabiee [i], Golnaz Heidari [k], Mahnaz Hassanpour [j], Ehsan Nazarzadeh Zare [l], Mohammad Reza Saeb [m,**]

[a] *Jiangsu Co–Innovation Center for Efficient Processing and Utilization of Forest Resources and International Innovation Center for Forest Chemicals and Materials, Nanjing Forestry University, 210037 Nanjing, China*
[b] *Department of Nutrition, Cihan University-Erbil, Kurdistan Region, 625, Erbil, Iraq*
[c] *Surface Reaction and Advanced Energy Materials Laboratory, Chemical Engineering Department, Amirkabir University of Technology, Tehran 1599637111, Iran*
[d] *College of Engineering and Technology, American University of the Middle East, Kuwait*
[e] *Department of Medical Biotechnology, School of Advanced Technologies in Medicine, Shahid Beheshti University of Medical Sciences, Tehran, Iran*
[f] *Department of Inorganic Chemistry, Faculty of Chemistry, Gdańsk University of Technology, G. Narutowicza 11/12 80-233, Gdańsk, Poland*
[g] *Department of Materials Science and Engineering, Pohang University of Science and Technology (POSTECH), 77 Cheongam-ro, Nam-gu, Pohang, Gyeongbuk 37673, South Korea*
[h] *School of Engineering, Macquarie University, Sydney, New South Wales 2109, Australia*
[i] *Biomaterial group, Department of Biomedical Engineering, Amirkabir University of Technology, Tehran, Iran*
[j] *Department of Chemistry, Institute for Advanced Studies in Basic Sciences (IASBS), Zanjan 45137–66731, Iran*
[k] *Department of Chemistry, Faculty of Science, University of Guilan, Rasht 41938-33697, Iran*
[l] *School of Chemistry, Damghan University, Damghan 36716-41167, Iran*
[m] *Department of Polymer Technology, Faculty of Chemistry, Gdańsk University of Technology, G. Narutowicza 11/12 80-233, Gdańsk, Poland*

ARTICLE INFO

Keywords:
Early diagnosis
Metal nanoparticles
Biosensors
Cancers
COVID-19

ABSTRACT

Early diagnosis is essential for the effective illness treatment, but traditional diagnostic approaches inevitably have major downsides. Recent advancements in nanoparticle-based biosensors have created new opportunities for accelerating diagnosis. High surface area, exceptional sensitivity, high specificity, and optical characteristics of metal and metal oxide nanoparticles have made it possible to detect a variety of health conditions and diseases immediately, including cancer, viral infection, biomarkers, and in-vivo imaging. Metal nanoparticles may be produced in a variety of ways, enabling the creation of innovative tools for chemical and biological sensing targets. The utilization of various metal nano-formulations, metal oxide nanoplatforms, and their composites in the early identification of illnesses is reported and summarized in this review. Additionally, the challenging corners in the use of metal oxide-based nano-scale diagnostic technologies in clinical applications are highlighted. The current work is believed to serve as a roadmap for in-depth research on inorganic nanomedicine, both *in-vitro* and *in-vivo* diagnosis of diseases and illnesses, especially pandemic infections like COVID-19.

* Corresponding author at: Department of Materials Science and Engineering, Pohang University of Science and Technology (POSTECH), 77 Cheongam-ro, Nam-gu, Pohang, Gyeongbuk 37673, South Korea.
** Corresponding author at: Department of Polymer Technology, Faculty of Chemistry, Gdańsk University of Technology, Narutowicza 11/12, Gdańsk 80-233, Poland
E-mail addresses: nrrabiee94@gmail.com, navid.rabiee@mq.edu.au (N. Rabiee), mrsaeb2008@gmail.com (M.R. Saeb).

https://doi.org/10.1016/j.onano.2022.100104
Received 5 September 2022; Received in revised form 7 November 2022; Accepted 8 November 2022
Available online 9 November 2022

Abbreviations: 3-3 4-dihydroxyphenyl propionic acid, (DHCA); 4-mercaptobenzoic acid, (MBA); Adamantane, (ADA); α-fetoprotein, (AFP); Amyloid β-protein, (Aβ); Branched polyethylenimine, (bPEI); B-type natriuretic peptide, (BNP); Cancer antigen, (CA); Carcinoembryonic antigen, (CEA); Cardiac troponin-T, (cTnT); Cell-free fetal DNA, (cffDNA); Cupric oxide, (CuO); Curcumin incorporated titanium dioxide nanoparticles, (CTNPs); Cyclic citrullinated peptide, (CCP); Cyclic strand displacement reaction, (SDR); Cyclodextrin, (CD); Dickkopf-1, (DKK1); dopamine, (DPA); Epigallocatechin Gallate, (EGCG); Electrochemiluminescence, (ECL); Enzyme-linked immunosorbent assay, (ELISA); Fluorescence resonance energy transfer, (FRET); Fluorescent Ag NPs-based immunoassay, (FSNIA); Fluorescent ZnO NPs linked immunoassay, (FZLIA); Folic Acid, (FA); Glassy carbon electrode, (GCE); Gold nanoisland, (AuNI); Graphene quantum dots, (GQDs); Graphene-poly(3-aminobenzoic acid), (GP-P3ABA); HCC: Hepatocellular carcinoma, (HCC); Epidermal growth factor receptor, (HEGFR); Hepatitis B, (HBV); Horseradish peroxidase, (HRP); Immunoglobulins, (IgG); Inductively coupled plasma mass spectrometry, (ICP-MS); Isoelectric point, (IEP); Lateral flow strip biosensor, (LFSB); Limit of detection, (LOD); Localized superficial plasmon resonance, (LSPR); Magnetic nanoparticles, (MNPs); Magnetic resonance imaging, (MRI); Magnetic-beads, (MBs)-; Malondialdehyde, (MDA); Microcapillary film, (MCF); Metal-enhanced fluorescence, (MEF); Microalbuminuria, (MAU); MicroRNA, (miRNA); Metal−organic framework, (MOF); Molecular imprinted, (MIP); N-Acyl-Homoserine Lactones, (AHLs); Nanoparticles, (NPs); Nanorod, (NR); Nanosheet, (NS); Neuron specific enolase, (NSE); Palladium, (Pd); Polyethylene glycol, (PEG); Photoacoustic, (PA); Photoacoustic tomography, (PAT); Photoluminescence, (PL); plasmonic photothermal, (PPT); Point of care, (POC); Polyamidoamine, (PAMAM); Polyaniline, (PANI); Polyethyleneimine, (PEI); Polymer diallyldimethylammonium chloride, (PDDA); Polymerase chain reaction, (PCR); Printed Circuit Board, (PCB); Prostate-specific antigen, (PSA); Quantum dots, (QD); Reduced graphene oxide, (rGO); Salivary a-amylase, (sAA); Single-photon emission computerized tomography, (SPECT); Superficial plasmon polarity, (SPP); Surface plasmon resonance, (SPR); Surface-enhanced Raman spectroscopy, (SERS); Single walled carbon nanotubes, (SWCNTs); Tetramethylbenzidine sulfate, (TMB); Thioflavin T, (ThT); Titanium dioxide, (TiO_2); Troponin-I, (cTnI); Volatile organic compounds, (VOCs); Zinc oxide, (ZnO)

1. Introduction

The overgrowth of the human population along with urbanization and industrialization has posed serious challenges to disease control. For instance, the recent pandemic and epidemic diseases caused by COVID-19 have become pervasive. Therefore, one of the enduring concerns of public health is the development of innovative materials, methods, systems, and technologies for an early-stage diagnosis of illnesses. Diagnostic strategies are of vital importance because they can make it possible to prevent the widespread prevalence of diseases, high mortality, and recurrence after treatment [1,2]. Early diagnosis can provide treatment opportunities for high-risk groups, and it seems the treatment of mounting diseases is effective only in the early stages of diseases [3] by modern technological methods such as DNA/RNA extraction [4,5] and sequencing [6]. For patients in the early stages, proper diagnosis and treatment can delay the growth of the disease and even the survival of the cancer patients. Researchers must thus undertake the necessary effort of developing technologies that can be employed for the sensitive and specialized approaches to diagnosis [7]. Early cancer detection, for instance, is essential to patients' effective treatment [8]. However, conventional diagnostic and imaging techniques have a poor capacity to distinguish between benign and malignant lesions due to their limited diagnostic capabilities and early identification [9,10].

The advancement of nanoparticles (NPs) with sizes between 1 and 100 nm is a focus of nanotechnology since it enables the creation of materials with distinctive structural/molecular architecture. With the help of these nanomaterials, the chemical, optical, and electrical properties could well be tuned [11,12]. In medicine, they provide the user with an effective nano-platform in order to construct the gene and drug delivery [13], as well as the diagnostics systems [14]. In the field of in vitro nano-diagnostics, nanotechnology has enabled the development of novel sensors, increased the sensitivity of current techniques, developed new diagnostic operating systems, and provided point-of-care programs [15]. NPs can provide more sensitive and selective detection of cancer and other disease [16,17]. Among various nanomaterials, metal and metal oxide have attracted a lot of attention due to their special structure and considerable mechanical, thermal, optical, and electrical properties [18]. Cost-effective metal NPs offer high sensitivity, prodigious specificity, and rapid disease diagnostic features [19,20]. Even at very low concentrations, metal and metal oxide NPs have a high potential for detecting illness biomarkers. Thus, they can increase the sensing characteristic of sensors as electrochemical biosensors [21] and optical devices [22,23].

Metal NP-based diagnostics are used to aid in the early detection of illnesses in people, preferably at the level of a single cell. Metal NPs' quick detection time, specificity, and sensitivity contribute to the development of a point-of-care mobile nanodevices [24,25]. Moreover, metal oxide nanomaterials have been integrated into biosensing systems due to their high adsorption capacity and improved electron-transfer kinetics. Because of factors such as surface charge and morphology, biosensing approaches based on metal oxide NPs rely on biomolecules' binding to these materials *via* chemical binding or physical adsorption [26]. Recently, various metals and metal oxide NPs such as gold, silver, palladium (pd), zinc oxide, cadmium sulfide, copper oxide, and magnetic NPs (MNPs) have been used in various sensors to improve biomolecule detection [27]. The MNPs, including spinel ferrites, has also become a promising candidate for detection tools at various levels [28] and the next stage of therapeutic purposes [29]. Along with MNPs, noble metals with a high surface area have inimitable physical and chemical properties that can improve the ultimate performance of biosensors for the sensitive detection of biomolecules [30,31] as well as in cancer therapy [32].

The effectiveness of metal-based biosensors in the future result of nanomedicine is dependent on overcoming a variety of technical hurdles ranging from theoretical studies of metal effects to standardization of biosensor production protocols. Some more challenges are associated with single-molecule detection. Besides, the development of biocompatible metal-based biosensors with minimum

toxicity is important for clinical applications, especially in the medical diagnostics [33,34]. The use of flexible technologies such as microfluidic systems has brought the capability to fabricate NPs with better control of size distribution, low sample consumption, and a high surface-to-volume ratio [35]. For example, the sensitivity of detection can be increased by using coupled metal NPs with point-of-care (POC)-based microfluidic systems and mobile devices. Microfluidics is the study of regulating extremely small fluid quantities in volumes between picoliters and microliters based on the management of multilayer fluid flow in small microchannels [35].

The use of metals, metal oxide NPs, and their hybrid or composite in electrochemical and optical biosensors for the early identification of illnesses is first summarized in this review. Then, the latest technologies which can be combined with biosensors to improve their performance and diagnostic sensitivity, are evaluated. Last but not least, the difficulties that will arise in using these biosensors are highlighted, along with potential solutions.

2. Fabrication methods for synthesis of metal-based nanomaterials

Metal-based nanomaterials are synthesized through top-down or bottom-up methods. The top-down method is based on mechanical size reduction through breaking down the materials into nanostructures. Bottom-up methods are based on assembling atoms to structure in a nanoscale range [36,37]. The top-down recommends the NPs preparation by sputtering, lithographic techniques, pyrolysis, etc. [36]. In these methods, there will be a deficiency in the surface engineering of the product and its derivatives, which is a significant limitation. However, the most known method to synthesize metal-based NPs is the bottom-up method, in which nanomaterials are grown from simpler molecules, and the size or the shape of the NPs can be controlled. Here, construction blocks of the nanomaterials are formulated first and assembled to yield the final NPs. Both chemical and biological techniques of metal-based nanomaterials depend on these methods [38].

Physical methods for the synthesis of metal and metal oxide-based NPs are considered due to their ease of modification, including laser ablation, UV irradiation, and sonochemistry [39,40]. During the physical synthesis procedure, the evaporation of metal atoms occurs, followed by condensation on different supports, in which the metallic atoms are aggregated as small clusters of metallic NPs. This method gives us nanomaterials with high purity. Although in this method, we need high energy consumption and advanced equipment. The absence of solvent contamination in the formed thin films and the uniformity of nanomaterials are the benefits of the physical synthesis method over chemicals [39]. Chemical synthesis methods that include thermal decomposition, micro-emulsion, mechanical procedures, chemical reduction, and etching are the common methods for the synthesis of metal nanomaterials, metal oxide nanomaterials and MOFs. The chemical reduction of NPs from their metal salt precursors through adding reducing agents is one of the most extensive methods of NPs synthesis [41]. Different reducing agents, such as formaldehyde, sodium borohydride ($NaBH_4$), and hydrazine, can be used during synthesis [42]. The chemical methods are economical for great-scale production, but toxic chemicals can cause environmental damage, thus limiting their clinical applications.

Green synthesis of metal-based nanomaterials is a method that is well-matched with green chemistry principles in which the molecules are prepared by using natural resources and can affect the performance of the final product. Among the green methods of synthesis of metal and metal oxide NPs, the use of plant extracts is simple and cost-effective to produce large-scale of NPs. The prepared nanomaterials have been considered to use in biomedical diagnostics, imaging, and molecular sensing [43]. The existence of different biomolecules, such as flavones, proteins, amino acids, alkaloids, polysaccharides, etc., in the plant has a significant role in the reduction of metals [44]. The difference in the morphology, size and properties of nanomaterials are controlled by differences in stabilizing and reducing agents, which usually plant extracts. Besides, green synthesis methods based on biological precursors depend on different parameters, such as pH, temperature, and solvent [43]. Under unique conditions, the quality of green synthesized

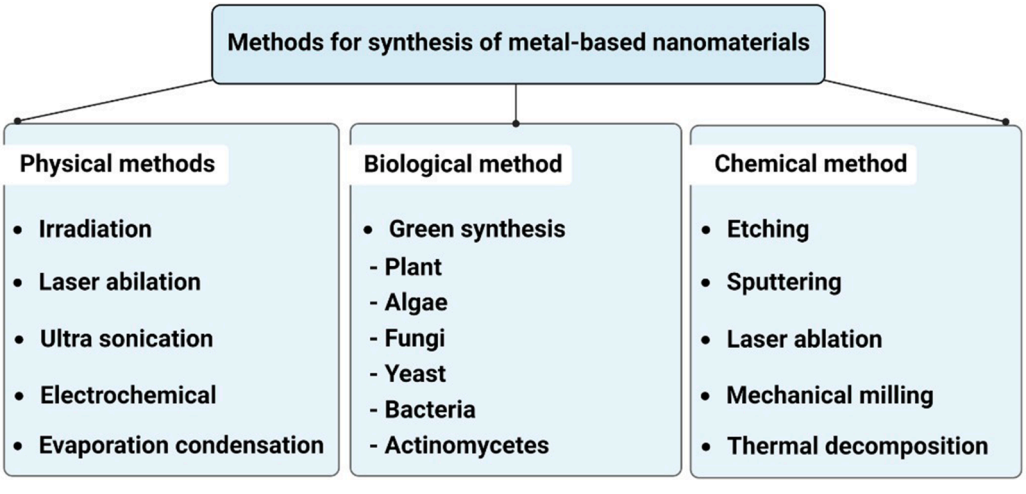

Fig. 1. Different biological, chemical and physical methods for the synthesis of metal-based nanomaterials.

metal-based NPs surpasses those manufactured through chemical methods. For example, in one study, the particle size of Fe_3O_4 NPs synthesized through the green synthesis method was 2–80 nm, which is much smaller than the 400 nm particles synthesized by the chemical method [45].Fig. 1 displays the different synthesis methods for synthesis of metal-based nanomaterials.

3. Metal NP-based biosensors

Biosensors have been developed in order to detection of a biological analyte by essentially converting a biocognitive event into a detectable and analysable signal. According to the working principle, the diagnostic elements used in biosensors can be DNA, antigens, antibodies, microorganisms, peptides, enzymes, aptamers, and ligands. Detection elements are immobilized by physical adsorption, covalent bonding, or trapping on the transducer surface. The transducer can be electrochemical, optical, calorimetric, and magnetic [46].

The optical characteristic of metal NPs depends on the surface plasmon resonance (SPR), which intensifies the coherent oscillation of free electrons on the metal surface in response to incident light. Depending on resonance and polarity, SPR can be a localized superficial plasmon resonance (LSPR) or a superficial plasmon polarity (SPP). As shown in Fig. 2, SPP originates from the propagation of waves along the metal surface, whereas LSPR happens when SP is confined to a volume smaller than the wavelength of incident light in order to metal NPs [47–49]. Environmental sensitivity of metal NPs and interparticle binding make it possible to use LSPRs in biosensing applications [50,51]. In addition, LSPRs can greatly amplify electromagnetic fields and make metal NPs suitable in order to use in surface-enhanced Raman spectroscopy (SERS) [52,53] and metal-enhanced fluorescence (MEF) [54]. To improve LSPR and make it appropriate for biosensor uses, size regulation of the noble metal nanomaterials is helpful. It is appropriate to choose suitable NPs sizes to attain greater detection sensitivity accordingly of greater shifts in response to RI changes according to the detection procedures. The plasmon shift per RI unit change is applied to designate the improved plasmonic sensitivity [55]. Different geometrical shapes of the metal NPs, such as triangular, stars, pyramids etc., have been described in order to optimum LSPR. In fact, the LSPR of triangular NPs, has been established to be more sensitive to RI changes according to their sharper tips or edges than other shapes since they produce hotspots with greater dipolar fields on their edges [56,57].

Other surface parameters, including diameter, morphology, periodicity, and excitation wavelength, can be made-to-order to acquire a high sensitivity than other materials in biosensors. The size and morphology of metal nanomaterials dependent energy stages are the provisos of metal nanomaterial's appropriateness in enhanced transduction circuitry. For example, cylindrical structures permit multiple interactions together and decrease the response time to a significant degree. Likewise, core-shell NPs provide a variation of conductance according to their insulated core and conducting shell [58]. Other surface properties, such as large surface area and good conductivity, can increase recognisers and receptor immobilization, electron transfer, and high sensitivity of biosensors [59].

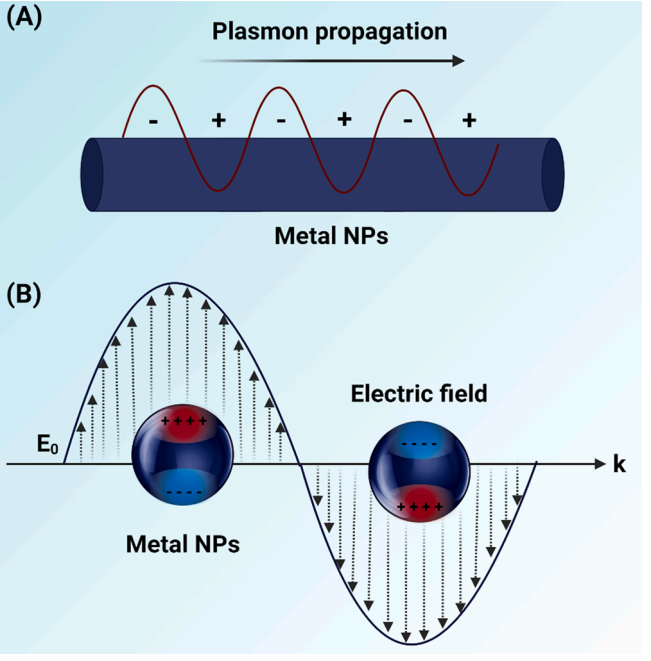

Fig. 2. (**A**) A simple illustration to introduce the surface plasmon polaritons and (**B**) the LSPR. Abbreviations: LSPR: Localized surface plasmon resonance.

Table 1
Various gold nanoformulation for the early diagnosis of disease.

Nanoparticle	Modifier or immobilization	Transducer	Size	Detection Limits	Diagnosis feature	Description	Ref
AuNPs	Citrate ligands	Optical	100 nm	At 4.0 ng/mL showed 90–95% sensitivity	Early-stage diagnosis of prostate cancer in blood	First, the absorption of tumor-antibodies to the NPs protein is done after binding the antigens, then a rabbit anti-human IgG is added to the solution to investigate the amount of IgG	[68]
AuNPs	Anti-PSA antibody	LSPR	25 nm	-	Highly sensitive detection of prostate antigen	A 25 nm colloidal AuNPs were conjugated with anti-PSA Ab, which LSPR was applied to detect the absorption changes of the NPs	[69]
Popocorn shape AuNPs	Anti-PSMA antibody	SERS	28 nm	-	Targeted diagnosis in LNCaP human prostate cancer cells	In the existence of LNCaP, popcorn-shaped Au NPs procedure different hot spots and offer a critical improvement of the Raman signal intensity	[70]
AuNPs	DTDTPA	-	~ 5.6 nm	-	Increase radio sensitivity of prostate tumors	DTPA was grafted onto AuNPs via thiol moieties, then with conjugation of Au@DTDTPA by gadolinium, simultaneously producing enhanced CT and MRI capability was occurs	[71]
AuNPs	Peptide probe	Electrochemical	14 nm	27 pg mL^{-1}	Determination of proteolytically prostate antigen in human serum	After immobilizing the peptide probe on the surface, AuNPs were connected to peptide thiol groups through self-assembly. After bonding the AuNPs, a strengthening step was done using silver enhancer solution. Then, the amount of deposited silver was measured by voltammetry	[72]
AuNPs	PEG- HER	Optical	-	-	Breast cancer cells	The attachment of PEG-thiol molecules to gold nanorods is done by their thiol functional group and the attachment of particles to Herceptin is done through Nanothinks Acid	[73]
AuNPs	anti-EGFR	SERS	15 nm	-	Oral cancer	The anti-EGFR –Au NPs by absorption of the antibodies onto its surface can be interact with cancer cells	[74]
AuNPs	ScFv EGFR antibody	SERS	60-80	-	Head and neck cancer	The immobilization of raman reporter, and a layer of thiol-PEG (thiol-PEG) on each 60-nm gold particle; The PEG layer also permits effective conjugation to tumor-targeting ligands	[75]
AuNPs	anti-IL6-IL-6 protein	Electrochemical		20−1000 pg/mL CEA, hEGR 10−200 pg/mL CA15-3	CEA, hEGR and CA15-3, lung cancer biomarkers	First, thiolation of the GID surface was performed using thiourea, then covalent attachment of Au NPs, blocking of the IDE surface (after antibody fixation) with ethanolamine, and antigen binding were performed	[76]
AuNPs	rProteinG	SPR	-	300 fM	Prostate specific antigen detection	First, rProtein G engineered at the C-terminus was developed to immobilize antibody molecules on the gold surface, then an immune reaction was generated after the absorption of monoclonal antibody against PSA	[77]
AuNPs	β-amyloid (1–40)	SPR	-	1 fg/mL	Alzheimer's disease	The immobilization of β-amyloid antibodies to -amyloid (1-40) on the Au surface was occurred, leading to a greatly efficient immunoreaction.	[78]
Au DENPs	FA, and fluorescein	-	-	-	Epithelial cancer	Au DENPs connected with FA and fluorescein isothiocyanate (FI). These FA- and FI- Au DENPs can connect to KB cells	[79]

Abbreviations: Surface-enhanced Raman scattering. DTDTPA: Dithiolated diethylenetriamine pentaacetic acid. HER: Herceptin. EGFR: Epidermal growth factor receptor. CEA: Carcinoembryonic antigen. CA15-3: Cancer antigen 15-3. HEGFR: Epidermal growth factor receptor. STM: Scanning tunneling microscopy . FA: Folic acid AuNP-based SERS probe was synthesized for early diagnosis of leukemic lymphocytes by capping AuNPs with a Raman reporter of 4-mercaptobenzoic acid (MBA) and antibody followed by encapsulation with polyethylene glycol (PEG) [80]. According to the raman characteristics data, the MBA in the AuNPs/MBA combination could demonstrate the SERS improvements associated with the MBA solution. In particular, it was determined that Raji cells labeled with anti-human CD19 antibody-conjugated AuNPs/MBA mixture and Jurkat cells labeled with anti-human CD3 antibody-conjugated AuNPs/MBA mixture could have the robust SERS signal, demonstrating that this SERS probe displayed the high specific and was appropriate in order to the diagnosis of leukemic lymphocytes.

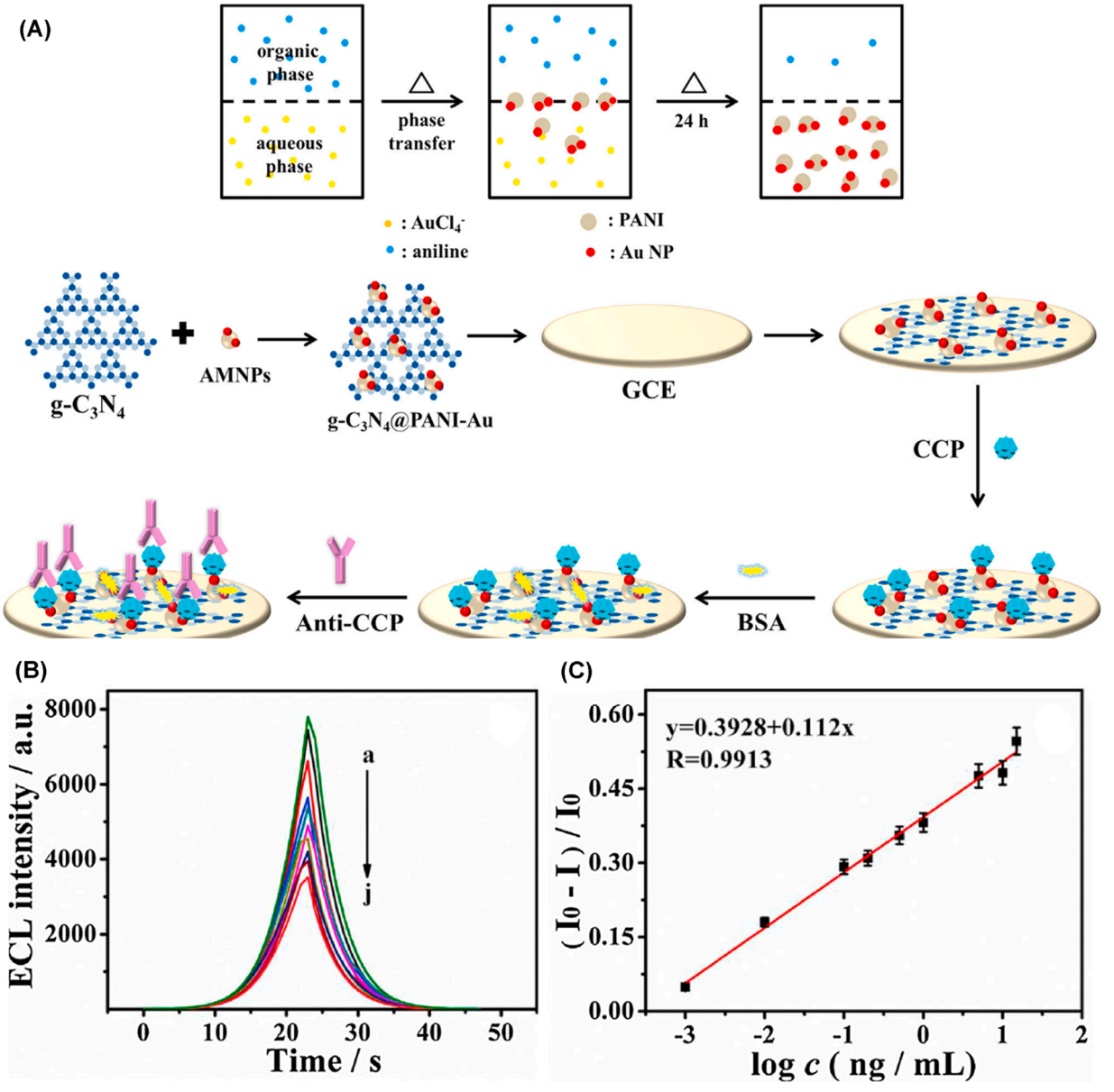

Fig. 3. (**A**) schematic preparation of PANI-Au ECL. GCE was polished into mirror using alumina slurry and washed with ultrapure water (**B**). ECL profiles of the immunosensor exposed to anti-CCP standards with different concentrations: the potential of 0.01–15 ng/ mL (a-j) in 1/15 mol/ L PBS containing 100 mmol/ L KCl and 50 mmol/ L $K_2S_2O_8$ (pH 7.0) (**C**) Calibration curve in order to anti-CCP determination. Reprinted with permission of Elsevier from Ref [81]. Abbreviations: PANI-Au: polyaniline-gold. ECL: Electrogenerated chemiluminescence. Anti-CCP: Anti-CCP. PBS: Phosphate-buffered saline.

3.1. Ag-based nanoparticles

Silver is one of the distinctive NPs with significant plasmonic characteristics. Owing to its unique electron transport and strong extinction bands, silver NPs often displayed substantial thermal and electrical conductivities [60]. Regarding stability, these NPs have demonstrated suitable stability in a variety of phases, like water and air [61]. Due to the significant optical properties and their band gaps, Ag NPs has been always considered as the promising nanoparticle for the early diagnosis and detection mechanisms in the optical biosensors [62]. They have less refractive index versus to the other NPs. When a biomolecule is attached to Ag NPs, it exhibits an increase in local refractive index and an Ag extinction shift. As a result, based on the changes that occur in Ag NPs, different sensors have showed the effective detection of target molecule [63]. Different physical and chemical approaches have been used to stabilize Ag NPs and used in different sensors such as, enzyme-linked immunosorbent assay (ELISA), surface plasmon resonance, Raman spectroscopy, and electrochemical biosensor to detection different biomarkers at greater sensitivity [64].

A fluorescent Ag NPs for diagnosis of HIV-1 p24 antigen in the early diagnosis of HIV is organized [65]. The fluorescent Ag NPs-based immunoassay (FSNIA) was shown to have a linear detection range among 10 and 1000 pg mL^{-1}. Also, false positives cannot be obtained from plasma samples of hepatitis B and hepatitis C and healthy adults (HIV^{-ve}) that didn't show any interference with diagnosis of HIV-1 p24 antigen.

An electrochemical sensor is established by modifying the glassy carbon electrode through the self-assemble of silver nanoparticle (inorganic nano-catalyst) and riboflavin-taurine (RFPT) (organic substrate) as diagnostic apparatuses in the diagnosis of malondialdehyde (MDA) in human real samples [66]. The RF-PT-Ag NPs platform demonstrated remarkable sensitivity in MDA detection by expanding the contact area with the MDA biomarker, which increased the electrochemical active sites to interact with MDA with a low LOD of 0.59 ± 0.05 μM.

The complete bacteriophage structure assembled to Ag NPs as a new SERS probe, was used to recognize the human promonocytic cell line U937 in vitro cancer cell model [67]. U937 cells targeted by the Ag network demonstrated the presence of novel RS peaks (862.6, 1132, and 1154 cm^{-1}) in addition to an increase in the intensity of several key U937 RS. Therefore, their prepared Ag–phage network could target cells and perform as signal reporters in the SERS spectroscopy.

3.2. Au -based nanoparticles

The use of Au NPs in biosensors based on optical and electrochemical processes is increasing due to the high sensitivity and selectivity that can be attained. In this context, Au NPs-based devices might be employed in POC devices to enhance trace-concentrations detections and diagnostics and boost targeted detection. Due to their controlled qualities, such as their forms, sizes, opto-electronic capabilities, and biocompatibility, Au NPs have therefore created the first ideal material for researchers (Table 1).

An electrogenerated chemiluminescence (ECL) sensor was developed by a dumbbell-like polyaniline-gold (PANI-Au) nanocomposite for detection of anti-cyclic citrullinated peptide antibody (anti-CCP) in order to the early diagnosis of rheumatoid arthritis (RA), as shown in Fig. 3 (A) [81]**.** Anti-CCP determination was shown to have a LOD of 0.2 pg/ mL. Compared to the previous work of anti-CCP, this study displayed a wider linear range response. (Fig. 3 B, C)).

AuNP- based pH-functionalized SERS biosensor chip LSPR was utilized for predicting critical complications in neurosurgical diagnoses. [82] The prepared biosensor enhanced the analytic concept about 3.29×10^9 factor with superior reproducibility and a LOD of 0.74 pM. In addition, it was indicated that five SERS-based biomarkers could offer significant information for the identification and prediction of SAH-induced cerebrovascular complication and hydrocephalus (91.1% confidence and 19.3% repeatability).

Various serum tumor markers containing carcinoembryonic antigen (CEA), Dickkopf-1 (DKK1), neuron specific enolase (NSE) and cytokeratin 19 fragment antigen (CYFRA21-1) were detected in cancer patients and healthy persons by gold NPs probes and microarrays in order to the diagnosis of lung cancer [83]. The proposed AuNPs probe can effectively detect multiple biomarkers with low concentration less than 1 ng/ mL in short time. Combined diagnosis of four tumor biomarkers enhanced the sensitivity of the lung cancer diagnosis to 87% in comparison with the sensitivity of individual markers.

Moreover, Au radioisotope NPs attached on graphene oxide sheets were prepared and used in order to *in vivo* single-photon emission computerized tomography (SPECT) imaging of tumors [84]. *In vivo* biodistribution of the Au NPs amino functionalized on graphene oxide nanosheets was studied in rats bearing fibrosarcoma tumor. The nanosheets presented a fast and excellent tumor uptake (with tumor to muscle uptake ratio of about 167 just 4 h after i.v injection), resulting in an effective tumor targeting. As a benefit, the nanosheets' low lipophilicity caused their rapid renal excretion in 24 h in the body, which reduced the likelihood of negative effects.

Streptavidin-labeled fluorescent AuNPs were made to develop immunoassays for the purpose of detecting HIV infection at an early stage [85]. The computational simulations using in silico investigations revealed that AuNPs can boost protein binding by increasing the interaction between certain active site residues and Au atoms. Glutathione coupled Au nanoclusters with streptavidin have a sensitivity limit of 5 pg/ml in order to detection of HIV-1 p24 antigen, which is thrice greater than the enzyme-linked immunosorbent test. More examples are provided in Supporting Information.

Some studies utilized the optical characteristics of AuNPs in order to the early diagnosis of COVID-19. For instance, a sensor system based on an enzyme-linked immunosorbent assay was created to recognize the nucleocapsid (N) protein related to SARS-COV-2. By using nucleic acid hybridization, a DNA probe made of gold nanoisland (AuNI) chips is created to match viral RNA sequences. Conjoining the LSPR and plasmonic photothermal (PPT) effect meaningfully improved the sensing sensitivity and stability. These nanoplatforms have the ability to identify N protein with a sensitivity of 0.22 pM, opening the door to potential medical diagnoses of COVID-19 patients in the early stages of infection [86]. Although, the sensitivity of a SARS-CoV-2 study has reported 3.7 RNA copies on

diagnosis of the RdRp sequence [87].

A rapid IgM-IgG combined antibody kit was established through a combination of gold NPs to diagnose SARS-CoV-2 [88]. The POC lateral flow immunoassay could identify antibodies simultaneously in contrast to the SARS-CoV-2 virus in human blood in a short time. Here, the antigen of SARS-CoV-2 can be anchored to antibodies conjugated to Au NPs and sprayed on pads. This test exhibited a sensitivity and specificity of 88% and 90%.

3.3. Cadmium Sulfide (CdS) nanoparticles

CdS NPs has good light-driven behavior and desirable bioactivity, which make it a good candidate for photocatalysis. CdS NPs, as prominent narrow-gap semiconductors, have enormous potential in photoelectrochemical bioassays [89,90]. CdS nanorod (NR) has recently received more attention because of its prominent photoelectrochemical activity which is attributed to its more photoactive sites and shorter radial carrier transmission distances [89–91]. A new photoelectrochemical biosensor was designed based on highly stable and photoelectrical active CdS nanorods modified with beta-cyclodextrin (β-CD@CdS NRs) in order to HIV DNA detection (Fig. 3) [92] . It was found that the prepared biosensor possesses high sensitivity, great stability, adequate feasibility in human serum samples and shows wide linear dynamic in the range of 10 fM – 1 nM with LOD of 1.16 fM, which this rate was lower than 15 fM in order to fluorescent assay through resonance energy transfer among Au NPs and carbon dots [93].

An ultrasensitive fluorescence immunosensor was developed based on greatly luminescent Polyamidoamine (PAMAM) dendrimers modified CdTe@CdS for diagnosis of Hepatitis B surface antigen (HBsAg) through monitoring fluorescence intensity [94]. The PAMAM dendrimer can covalently attach to CdTe@CdS via its functional amine groups and magnify the fluorescence signal of QDs, increasing sensitivity. The designed immunosensor presented outstanding analytical performance under optimal conditions for detecting of HBsAg in a linear range of 5 fg/ mL - 0.15 ng/ mL with LOD of 0.6 fg/ mL. This immunosensor showed a broader linear range and a lower LOD to HBsAg detection [95,96].

A high sensitive photoelectrochemical biosensor based on the molecular imprinted (MIP) polydopamine-coated CdS/CdSe was reported for detection of L-phenylalanine as phenylketonuria biomarker [97] . It was indicated that the prepared PEC biosensor

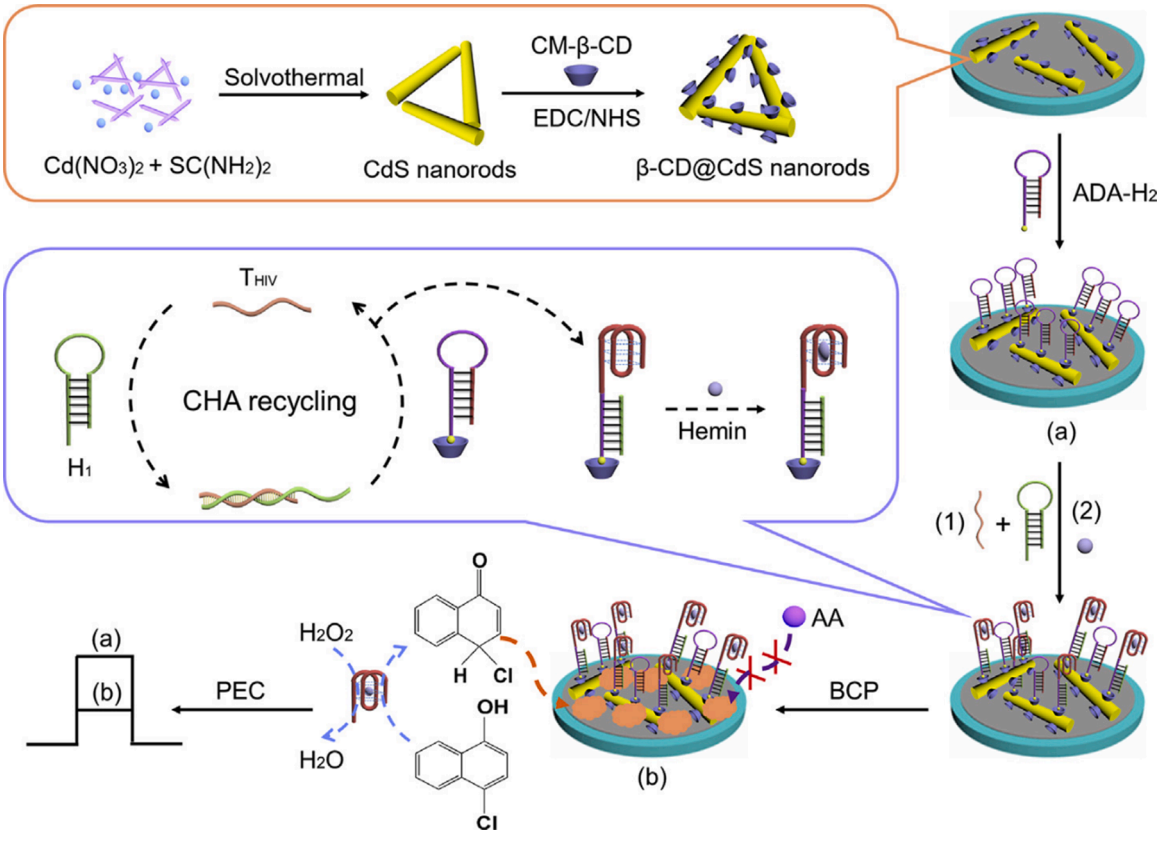

Fig. 4. Schematic show of synthesizing of β-CD@CdS NRs and stepwise assembly procedure in order to photo electrochemical assay of HIV biomarker based on CHA-mediated enzymatic reaction. This β-CD@CdS NRs perform as signal element in order to photocurrent production, as well as immobilize adamantine-labeled hairpin DNA2 (ADA-H2) probe by host-guest interaction. Reprinted with permission of Elsevier from Ref [92]. Abbreviations: β-CD@CdS NRs: Beta-cyclodextrin-functionalized CdS nanorods. CHA: catalytic hairpin assembly. ADA: Adamantine. ADA-H2: adamantine-labeled hairpin DNA2.

showed greater capability for detection of L-phenylalanine biomarker which resulted in two linear range 0.005–2.5 and 2.5–130 μM at the optimized condition with LOD of 0.9 nM. More examples are provided in Supporting Information.

3.4. Pd-based nanoparticles

Pd NPs (PdNPs) have ultrathin structure, high photothermal efficiency and catalytic properties which make them an ideal candidate for imaging enhancement in early diagnosis [98]. Recently, some researchers have reported the use of Pd for optical diagnostic imaging.

Ultra-sensitive, unlabeled electrochemical biosensors were developed for detection of microRNA (miRNA) using PdNPs [99]. The results revealed that the Pd-based biosensor detect miRNA-21 in the linear range of 50 aM–100 fM with limit of detection of 8.6 aM. In addition, the prepared Pd-based biosensor demonstrated high stability, excellent reproducibility and possibility for detection of miRNA-21 in serum samples which guarantees this biosensor in the detection of the disease. Pd nanosheets was used as exogenous photoacoustic (PA) contrast agents according to its high optical absorption in the near-infrared region [100]. An important and long-lasting imaging increment in SCC7 squamous cell carcinoma of the head and neck was observed by photoacoustic tomography (PAT) after administration of Pd nanosheets in mice. It was indicated that the morphology and functional perfusion of the tumors were delineated due to the accumulation of Pd nanosheets in the PA images.

PdNPs having the same catalytic activity as a horseradish peroxidase (HRP) mimic enzyme were proposed for efficiently catalyzing the H_2O_2-mediated oxidation of 3,30,5,50-tetramethylbenzidine sulfate (TMB), which can alter the color of solution from colorless to blue [101]. Thereupon, very sensitive sarcosine detection can be achieved by eye observation and ultraviolet spectrophotometry in the LOD of 5.0 nM which shows higher sensitivity and better analytical activity than other biosensors [102]. As shown in Fig. 5, an

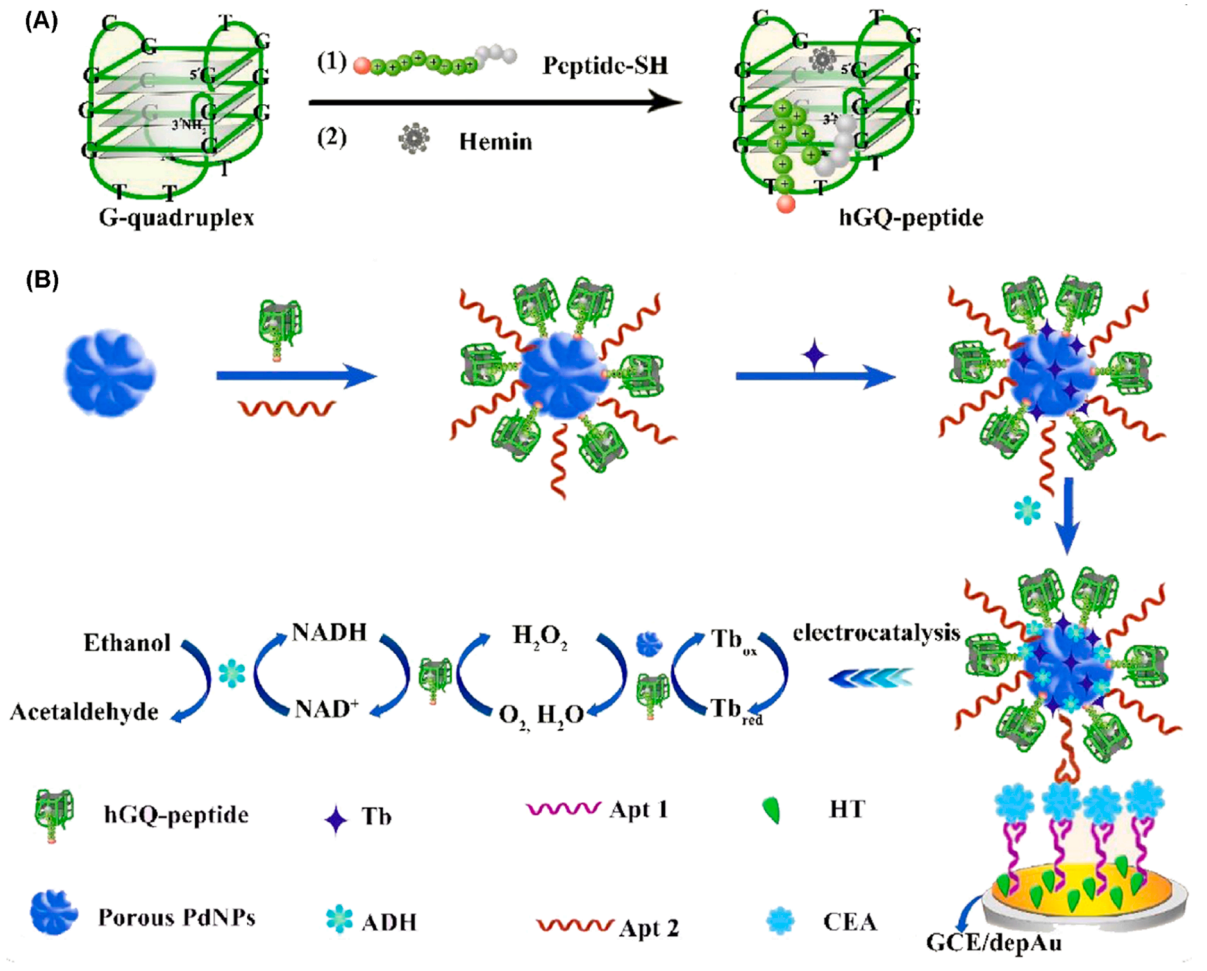

Fig. 5. (**A**) Schematic preparation of hGQ-peptide DNAzyme and (**B**) Boosted electro-catalysis of hGQ-peptide together with the CEA detection mechanism. Here, according to the high surface area, porous palladium performed as matrix in order to co-immobilization of the hGQ-peptide hybrid, aptamer, redoxactive Tb and ADH. Reprinted with permission of Elsevier from Ref [103]. Abbreviations: hGQ-peptide: Hemin/G-quadruplex. Tb: Toluidine blue. ADH: Alcohol dehydrogenase.

electrochemical aptasensor is used to detect carcinoembryonic antigen (CEA) applying the porous PdNPs attached to hemin/G-quadrupole-bound peptide and conjugated with peptide (hgQ-peptide) [103]. The developed aptasensor showed CEA determination with LOD of 20 fg/mL which displayed ultrasensitive detection capability for clinical diagnosis than related prior electrochemistry biosensor [104].

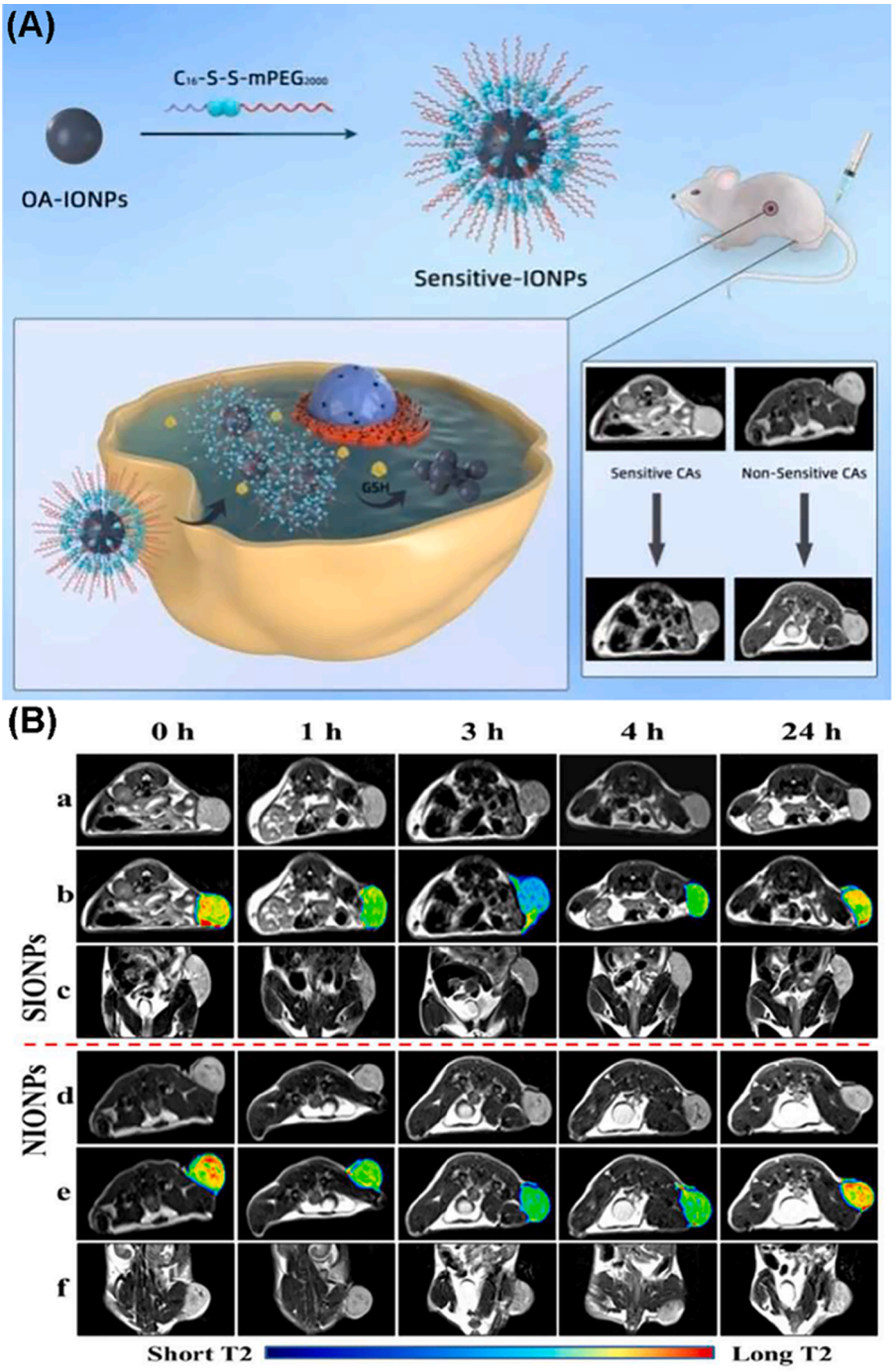

Fig. 6. (**A**) The reduction-activated MRI probe SIONPs and the mechanism in order to reduction-triggered MRI improvement in order to cancer diagnosis (**B**) (a-f) T2-weighted imaging (a, d), pseudo-color images (b, e) coronal MR images (c, f) C6 tumor-bearing mice at a programmed time after intravenous. Reprinted with permission of Elsevier from Ref [108]. Abbreviations: SIONPs: Superparamagnetic Fe_3O_4 NPs. MRI: Magnetic resonance imaging.

4. Metal oxide NP-based biosensors

4.1. Iron oxide-based nanoparticles

Fe_3O_4 possesses promising features including high stability, excellent biocompatibility, and good strengths, which make it a good candidate as a magnetic resonance imaging (MRI) contrast agent. Iron oxide-based contrast materials minimize relaxation time, resulting in a low signal in the weighted image. The use of magnetic NPs (MNPs)-based MRI allows for the early diagnosis or monitoring of numerous illnesses such as inflammatory diseases and cancer.

The development of carboxyl decorated Fe_3O_4 NPs was reported for MRI as an important diagnostic tool because of its noninvasive and tomographic capabilities. [105]. The prepared carboxylated Fe_3O_4 NPs with the size of 10 nm showed high colloidal stability and high resistant to adsorption of protein in physiological medium. T2-weighted MRI scan of the iron oxide NPs in the water provided a transverse relaxation value of 215 $mM^{-1}s^{-1}$. The synthesized carboxyl decorated Fe_3O_4 NPs with excellent colloidal stability and high transverse relaxation value become a hopeful candidate in high performance MRI contrast agent for diagnosis application. Natural rubber latex coated Fe_3O_4 NPs was synthesized and employed as a MRI contrast agent [106]. The MRI results exhibited that enhancing

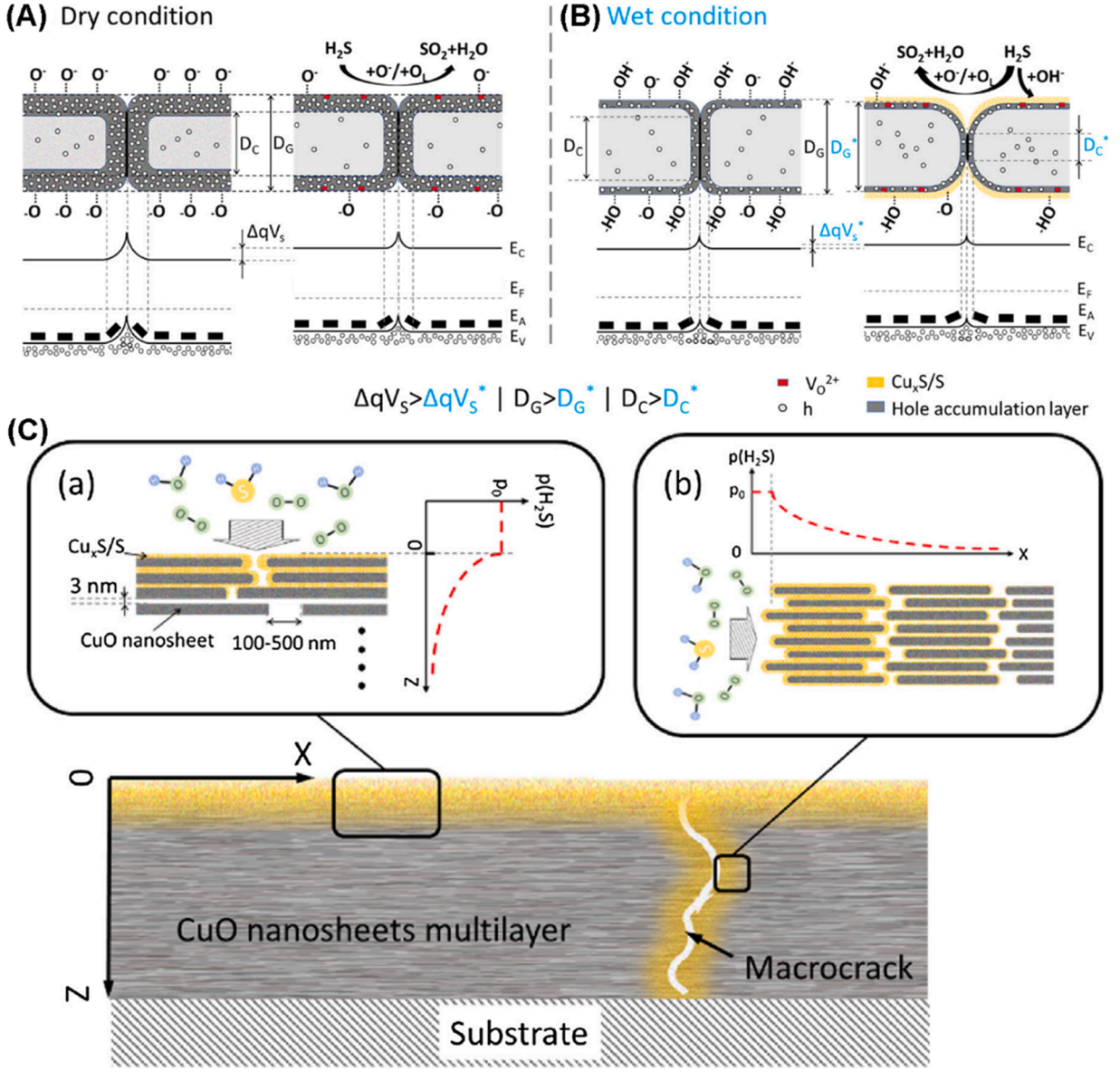

Fig. 7. Molecular and mechanistic views of CuO nanosheet sensing layer for (**A**) dry and (**B**) humid conditions. (**C**) CuO nanosheet sensing film in humidity comprising H_2S. Reprinted with permission of Elsevier from Ref [119]. Abbreviations: H_2S: Hydrogen sulfide.

the concentration of natural rubber latex reduced R2 relaxation and the relaxation ratio of r2/r1 of MNPs considerably.

Particles of Fe_3O_4 NPs functionalized with carboxyl modified PEG by a dopamine (DPA) linker were used as contrast agents in MRI to detect breast cancer [107]. The findings showed that enhancing the concentration of NPs from 12 to 312 mg/ L decreased transverse relaxation, which in turn enhanced the MR signal. A differential detection method was also developed for non-invasive glioma imaging based on an activation strategy to reduce the intracellular accumulation of superparamagnetic sensitive Fe_3O_4 NPs [108]. *In vitro* (HUVEC cells, BMSC cells, MCF-7 cells, CT26. WT cells, C6 cells, 4T1 cells, and Hela cells) magnetic resonance imaging showed that Fe_3O_4 NPs could effectively enhance the T2 relaxation rate and MR imaging in tumor with redox microenvironment through accumulation of responses at the tumor site. *In vivo* experiments on C6 xenografted tumor nude mice displayed that the enhancement of contrast imaging with T2-weight could be utilized in various inflammatory mass and malignant glioma (Fig. 6).

The synthesized Folic Acid (FA) modified Fe_2O_3 NPs were shown to have good colloidal stability [109]. It was indicated that, in vitro MRI test of FR-deficient embryonic kidney cells (HEK 293) and folate receptor (FR) cancer cells (HCT 116) demonstrated the target specificity of the FA-Fe_2O_3 NPs relative to the cancer cell, so the contrast agent MRI is pronounced for diagnose colorectal cancer. Biocompatible FA modified albumin-dextran-Fe_3O_4 NPs (Fe_3O_4/BSA-DEX-FA) were prepared [110]. The synthesized nanoformulation with the size of 100 nm showed proper stability, good transversal R2 relaxation rate, and magnetically guided functions. It

Table 2
Various metal oxide NPs for the early diagnosis of different disease.

Nanomaterials	Modified or immobilization	Transducer	Size	Detection limit/ Sensitivity	Diagnosis features	Description	Ref
Iron oxide NPs	FA	Optical	23 nm	Separation efficiency of 61.3%	Early diagnosis of ovarian cancer cells	FA-PEG-NH2 was immobilized to the IO NPs, then the IO–FA NPs were connected to the surface of cancer cells	[138]
Fe_3O_4 NPs	Oleylamine	-	7.5 nm	-	Early detection of malignant glioma	First, the formation of NPs assembled from the mono methoxy-poly-(ethylene glycol)-S-S-hexadecyl (mPEG-S-S-C16) and oleic acid -Fe3O4	[108]
ZnO	Anti-HRP2	Electrochemical	-	6 attogram/ ml	Detection of Histidine-rich protein-2 related to Malariadisease	Antibodies were connected to functionalized Cu-doped ZnO nanofibers [fCZnONF] using EDC-NHS crosslinking chemistry.	[139]
ZnO	ZIKV-NS1 antibody	Electrochemical		1 pg/ mL	Early and rapid detection of ZIKV infection	The antibody was immobilized on the ZnO surface by glutaraldehyde and cystamine	[129]
ZnO	$A\beta_{42}$ peptide	Fluorescence		12 ag/ mL	Early detection of Amyloid-beta 42 ($A\beta_{42}$)	The immobilization peptide (P2) occures on the ZnO nanoporous. After the sample added, . the sample signals were detected using fluorescence microscopy	[132]
SnO2 and ZnO	-	-	146nm	High	Early detection of lung diseases	The sensor was measured VOCs analytes using its response time and voltage changes.	[140]
CuO	MnAl LDHs	Electrochemical		0.126 μM	Real time detection of H2O2from blood serum	The immobilization of MnAl LDH to CuO by attaching CuO NPs with MnAl LDHs by a co-precipitation, for H_2O_2 reduction for biological uses	[141]
CuO	DNA	Colorimetric	13 nm	0.64 nM	Detection of single nucleotide polymorphism	DNA absorbed to the CuO NPs and its capability to bind to dsDNA	[118]
SiO_2	-	Electrochemical	115 nm	0.03 ng/mL	Detection of prohormone BNPT in order to acute myocardial infarction in human serum samples	Electrode can be coated with SiO_2@Ir to modify capture antibodies based on the reaction among the NH_2 groups on SiO_2@Ir and carboxyl groups on the antibodies. Finally, the detection of BNPT occures by biosensor	[142]
CuO	Streptavidin		9 nm	1.0 nM.	Rapid detection of HPV16 DNA Within 20 min	First, CuO NPs was coated through streptavidin, then the probe DNA was modified on CuO NPs' surface through biotin-streptavidin.	[123]

Abbreviations: LDH: Layered double hydroxid. BNPT: Brain natriuretic peptide. HPV: Human papillomavirus. VOCs: Volatile organic. BNPT: Brain natriuretic peptide compounds. Folic acid: FA

was observed that Fe_3O_4/BSA-DEX-FA NPs could remarkably enhance the tumor MRI of KB tumor-bearing mice.

In another study, dextran-functionalized graphene oxide nanosheets were decorated by superparamagnetic iron oxide NPs and applied for positive contrast MRI application [111]. The benefit is that, at dosages two orders of magnitude lower than those typically applied in order to Magnevist®, the synthesized nanomaterials could offer the same contrast to noise ratio.

4.2. CuO-based nanoparticles

Copper is a noble metal alternative because of its notable benefits such as low cost, non-toxicity, strong electrochemical activity, and the ability to perform amperometric measurements under alkaline circumstances [112–114]. Accordingly, the behavior of copper in biosensor for early diagnosis of diseases has been widely studied through various research groups according to the probability of

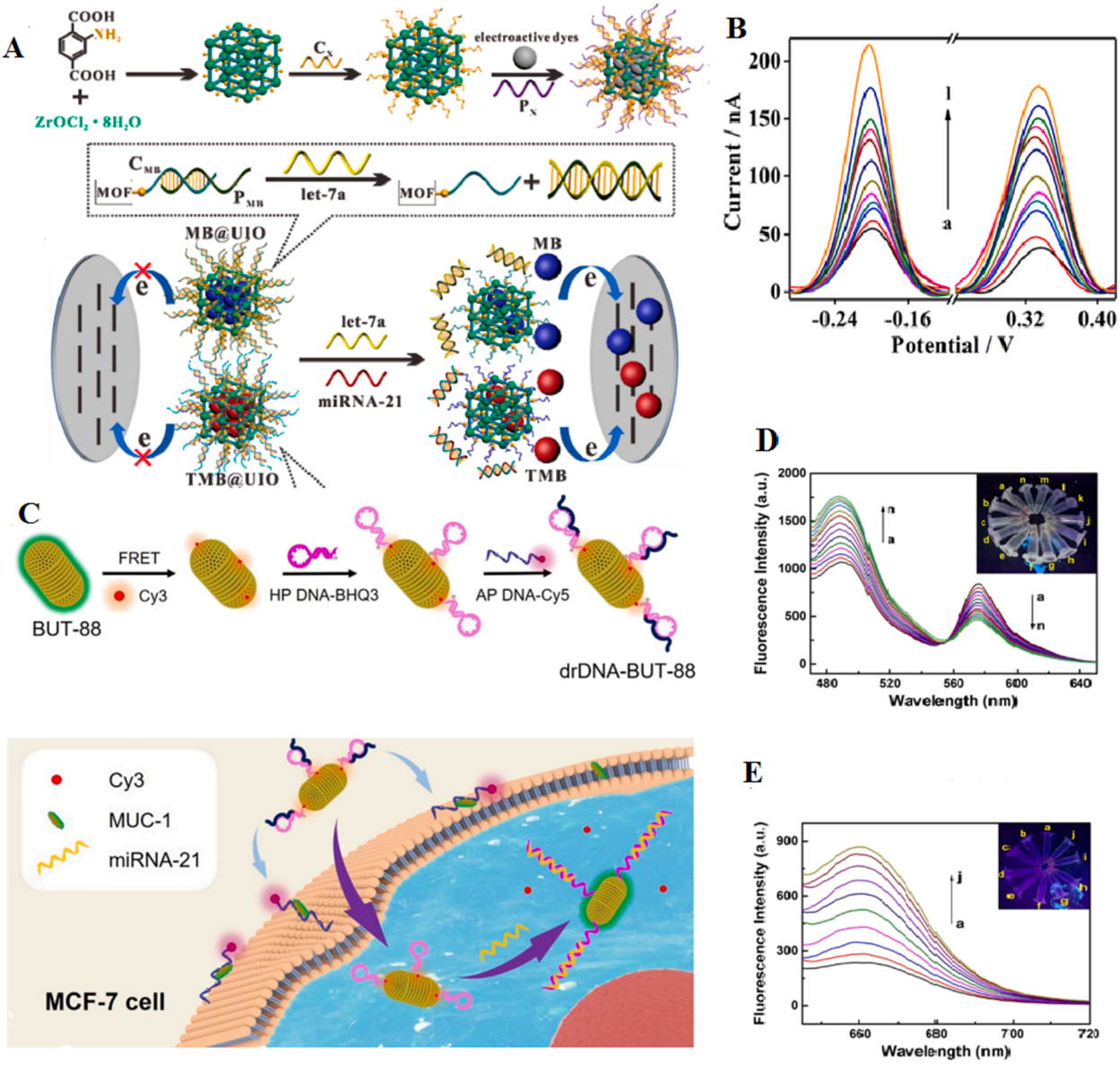

Fig. 8. (A) Schematic illustration of the Nucleic Acid-modified MOFs formation process and the attitude of the MOF-based electrochemical biosensor to multiple detections of miRNAs. (B) The DPV shows the biosensor matching to let-7a and miRNA-21 with various concentrations, which compared with that of the MB@UIO and TMB@UIO, the DPV enhanced visibly with the let-7a and miRNA-21 concentrations enhancing, which could be responsible for the sensing value that more target analytes triggered the release of more dyes [148]. (C) fabrication of the drDNABUT-88 probes and specific detection of MUC-1 and miRNA-21 in MCF-7 cells. (D) Fluorescence spectra of BUT-88 and Cy3 in the existence of various concentrations of miRNA-21 (0, 0.2, 0.4, 0.6, 0.8, 1.0, 2.0, 4.0, 6.0, 8.0, 10, 20, 60, and 80 nM). (E) Fluorescence spectra of Cy5 in various concentrations of MUC-1 (0, 8, 10, 20, 40, 60, 80, 100, 200, and 400 nM) [149].

Table 3
Application of various nanoformulation in early diagnosis of disease.

Nanoformulation	Modifier or immobilization	Transducers	Size	Detection Limits	Diagnosis	Description	Ref
Cuprous oxide @ ceric dioxide/AuNPs	as transducing materials modified GCE.	Electrochemical	-	0.1–100 ng/ mL (LOD of 0.03 pg/ml)	Detection of prostate specific antigen in human serum	The immobilization of Cu_2O@CeO_2-Au onto the surface of GCE enhance the surface area to capture a antibodies in order to detection of PSA	[155]
Graphene oxide/AuNP	ERBB2c and CD24c DNA	Electrochemical	-	Detection limits of 0.16 nM and 0.23 nM for ERBB2 andCD24, respectively.	Early diagnosis of breast cancer biomarker	ssDNA on AuNPs-GO grafted on GCE g Immobilized by π–π stacking interaction that can develop an electrochemical detection in order to ERBB2 and CD24	[156]
SWCNT-grafted dendritic Au/ Cd^{2+}	**PNA probe**	Electrochemical	-	0.01 fmol L^{-1}	Detection of miR-21 for early diagnosis of prostate cancer	The immobilization of thiolated probes was performed on den-Au nanostructures through the SAM process. Then miR-21 and Cd^{2+} ions signal was measured by voltammetry techniques	[157]
Echinoidea-shaped Au@Ag-Cu_2O	Ab1 and Ab2	Electrochemical	-	0.003 pg/mL	Highly sensitive determination of prostate specific antigen	Au@N-GQDs was applied to successfully immobilize Ab1, then the Au@Ag-Cu2O NPs were used to capture Ab2 and used for H_2O_2 reduction to amplify the recognition signal	[158]
Cu ion loaded porous-hollowed-silver-gold core-shell NPs	Anti-PSA	Electrochemical	64.83 ± 5.11 nm	0.13 pg/mL and 4 orders of magnitude better than the clinically relevant level in human serum.	The electrochemical sensors used for detection of prostate cancer.	First, PSA antibody Immobilized on the electrode, after added PSA target molecules, with immobilization of (Cu2+- PHSGNPs-Anti-PSA2 on the surface of electrode, electrochemical measurement of reaction was done	[159]
Au beads and platinum NPs	HRP		-	LOD of 0.005 mU L^{-1} which is 100-fold lower than that of commercial enzyme immunoassay	Early diagnosis of thyroid cancer	HRP was immobilized on platinum NPs by the electrostatic interactions among NPs and NH_2 of HRP	[160]
Fe_3O_4/Aucore/shellNPs	Single stranded DNA(ssDNA)	Fluorimetric	-	In the linear rangr of 1.6×10^{-15} to 6.6×10^{-13} M with detection limit of 1.2×10^{-16} M	Early diagnosis of methylation dependent diseases such as cancers.	First, Fe@Au NPs modified by bounding of ssDNA probe through sulfhydryl group, then unmethylated and methylated complementary target ssDNA were hybridized with the immobilized ssDNA probe. With adding of the target, fluorescence intensity was measured	[161]
ZnGeO:Mo persistent luminescence nanorods and Au@Ag@SiO_2	-	ElectrochemicalSERS	44.9 ± 2.6 to 74.1 ± 4.0 nm	9.2 pg/ mL	Early diagnosis of malignant cancer	Quantitative diagnosis of uric acid in order to quick detection of early preeclampsia by electrochemical SERS is developed	[162]
La(III)- MOFand Ag NPs	Aptamer	Fluorescent	-	0.04 ppb (ng/mL) or 5.5 fM of the miRNA-155 biomarker	Lung and breast cancer diagnosis	First, probe 1 and 2 are connected to La(III)-MOF and Ag NPs, respectively. By adding miRNA-155 to a mixture of probe-1 and probe-2 according to the amount of miRNA and Active sites, hybridization reaction and FRET process occurs	[163]
CuO/ZnO	-	Colorimetric / fluorescence	Average diameter of ≈10 nm length of 25–50 nm.	40 1 μM (4.8 μg/ mL)	Detection of Cys and Hcy	The interaction among the Cys and platform effects on the electron reduction of Cu(II) to Cu(I) causing to the formation of a complex among Cu(I) and Cys	[164]
Mn-doped ZnO	-	Electrochemical	~15–20 nm	0.35 nM	Myocardial Infarction		[165]

(*continued on next page*)

Table 3 (*continued*)

Nanoformulation	Modifier or immobilization	Transducers	Size	Detection Limits	Diagnosis	Description	Ref
						Detection of 3–15 nM Mb biomarker in order to myocardial infraction at early stage using electrochemical method	
CdS-Cu_2O nanorod on Ti mesh	Aptamer	Photoelectrochemical	-	Linear range of 0.1–100 ng/·mL and detection limit of 0.026 ng/·mL	PSA detection	After the immobilization of aptamer on the surface of CdS-Cu_2O NAs/TM, increased photocurrent can be attained in the existence of PSA according to the specific binding of the aptamer to PSA	[166]
Au/CdSNH_2GO	Monoclonal antibodies (IgM)	SPR	-	0.1 pM	Dengue virus E-protein sensing	CdS-NH_2GO were modified with monoclonal antibodies (IgM) based on SPR optical sensor in order tor diagnosis of dengue virus (DENV) E-protein	[167]
CdS QDs functionalized polystyrene microspheres(PS) and graphene oxide(GO) -polyaniline(PANI)	Polystyrene and polyaniline	Electrochemical	CdS QDs 1.6 nm	3 cells mL^{-1}	Detection of K562 cell	According to the electrostatic force, the PDDA and CdS QDs were assembled on the surface of polystyrene microspheres, then the structure enhanced the detection signal intensity	[168]
TiO_2/CdS/CdSe	anti-IL-6 antibody		CdSe QD 2.81 nm TiO_2 22-28 nm	Wide linear range of 1.0 pg/mL-100ng/mL low detection limit of 0.38pg/mL	humaninterleukin-6 (IL-6)	After attaching TiO_2/CDS on an ITO electrode, chitosan was coated on the surface by the coordination effect of hydroxyl and amino groups with Cd_2þ ions, then, IL-6 was detected through the immunoreaction of IL-6–CdSe and IL-6 with anti-IL-6 antibody	[169]
CuO/MWCNT	human IgG, goat-antihuman IgG	Chemiluminescence	24.2–33.2 nm	Linear range of 3.5×10^{-9}–2.5×10^{-6} and 2.2×10^{-9}–5.0×10^{-6} g ml^{-1} with LOD of 1.8 and 0.85 ng ml^{-1} for CuO and CuO/MWCNT, respectively.	Detection of HBs Ag for diagnosis of infection.	Antibody has been effectively adsorbed by covalent bonding on the CuONPs and MWCNT/CuONPs surfaces, then secondary antibody react with antigen to that observed by chemiluminescence	[170]
Graphene quantum dot-Pd@Au	Folic acid and glutamic acid	Electrochemical	-	In the range of $3-1 \times 10^5$ HepG2 cells mL^{-1} with LOD of 2 cells mL^{-1}	Detection of circulating cancer cells in human blood	FA/GluGQD powerfully connect with cancer cells to foem target detection	[171]

Abbreviations: LOD: Limit of detection. $ERBB_2$: Human epidermal growth factor receptor 2. SWCNTs: Single walled carbon nanotubes. Cd^{2+}: Cadmium ions. Ab: Antibodies. GQDs:Graphene quantum dots . HRP:Horseradish peroxidase. Cr^{2+}: Chromium. rGO: reduced graphene oxide. MOF: metal−organic framework. ZnO-NGQDs: Zinc oxide-nitrogen doped graphene quantum dots. Cys: cysteine. Hcy: Homocysteine. PSA: Prostate-specific antigen. CEA: Carcinoembryonic antigen. DNA MTase: DNA methyltransferase . HBs Ag: Hepatitis B surface antigen. GCE: Glassy carbon electrode. SAM: Self-assembly monolayer process

producing cupric oxide (CuO) in order to permit rapid oxidation of carbohydrates [115,116].

A CuO film was placed on a Cu electrode through thermal and chemical treatment for demining salivary a-amylase (sAA) in saliva samples by detecting maltose produced via enzymatic hydrolysis of starch for chronic periodontitis diagnosis [117]. Detection of a maltose was obtained in the range of 0.5–6.0 mmol/ L and the LOD of 0.05 mmol/ L. Therefore, their offered assay is cheap which can provide reliable information in a very short time without requirement of sophisticated instrumentation.

CuO was applied to identify SNP in cell-free fetal DNA (cffDNA) [118]. The peroxidation activity of CuO in the existence of DNA enhanced in comparison with single-stranded DNA. It was indicated that the increment of peroxidation activity is the basis in order to detection among nontarget, and sequences. The linear detection range was observed at 2–12 nM with LOD of 0.64 nM which can establish the procedure of diagnosing sickle cell anemia.

The self-assembled CuO nanosheets [119] were employed for monitoring H_2S concentration which known as biomarkers of halitosis [120], small intestinal bacterial overgrowth (SIBO) and asthma [121,122]. The mechanism of the CuO gas sensor in dry/ humid conditions is compared in Fig. 7 (A and B). In the humid environment, oxygen anions are replaced by hydroxyl groups, which affects reactions among oxygen atoms and H_2S. Therefore, the signal to H_2S reduced as the humidity level improved. Furthermore, the greater humidity level caused in an abundance of terminal hydroxyl groups, thus, higher conversion from CuO to Cu_2S and S happened. This study showed that CuO nanosheets have constant response to H_2S with coefficient of variations less 3 %, irrespective of humidity changes. The prepared sensor displayed superior sensitivity with LOD of 3 ppb for detection of H_2S. As a result of its excellent diagnostic sensitivity, especially in high humidity conditions, this sensor can be widely employed in the creation of environmental diagnostic sensors and even respiratory analysis [119].

CuO was applied as colored tags in lateral flow strip biosensor (LFSB) in order to detection of human papillomavirus type 16 (HPV16) which is responsible for cervical cancers [123]. It was observed that CuO-based LFSB have excellent ability in detection of HPV16 DNA with a LOD of 1.0 nM. In addition, the CuO capture probes indicated outstanding stability and reproducibility.

The copper oxide nanomaterials, as one of the effective antibacterial nanomaterials [124] with capability of redox interaction with bacteria during their respiration resulting in some glycolysis process, can be applied as highly sensitive and rapid response self-sterilizing biosensors [125]. The response time of the biosensor were found as low as about 2 min. Thus, the LOD of the sensor was reported to be about 10^2 colony forming unit per milliliter for Escherichia coli bacteria. Meantime, the bacteria could not survive on the surface of biosensor, showing its self-sterilizing property. In this regard, after 30 min, 88% and 97% of the bacteria were inactivated in the dark and under light irradiation, respectively.

4.3. ZnO-based nanoparticles

Zinc oxide (ZnO) has been extensively known as a transduction material for biological sensor advancement because of its high isoelectric content, biocompatibility, and other multifunctional properties. The attractive properties of ZnO aid maintain the biological activity of immobilized biomolecules and enhance sensing performance. The high surface area of ZnO nanostructure provides signal amplification to detect target biomarkers by increasing sensitivity and selectivity. ZnO has an isoelectric point (IEP) of 9.5, which is greater than the IEP of most biomolecules and therefore offers an exclusive matrix for the immobilization of biomolecules. Biomolecules have negative charge at physiological pH because of less IEP, so positively charged ZnO can easily immobilize them via strong electrostatic interactions [126]. ZnO's ionic and semiconductor characteristics can help achieve maximum sensitivity for diagnosing target biomarkers at ultralow concentrations. ZnO can be produced with current volume scalable techniques at low cost [127,128]. Therefore, it is possible to develop ZnO based biosensor with low-cost as portable micro device, which is essential for POC diagnostics. Recently, many researchers have studied ZnO nanostructures for biosensing applications is early diagnosis disease.

An electrochemical immunosensor were developed using ZIKV-NS1 antibody immobilized ZnO nanostructures on Printed Circuit Board (PCB) for early diagnosis of Zika infection [129]. The portable designed biosensor is inexpensive and simple, allowing quick Zika virus detection in undiluted urine within a linear range of 0.1–100 ng/mL, and making it a suitable choice in order to POC applications. The LOD was found to about 1 pg/mL, showing that the ZnO -based immunosensor is a virtuous quick test in order to recognition of ZIKV at the beginning of the disease.

Streptavidin labelled fluorescent ZnO NPs was employed for development of fluorescent ZnO NPs linked immunoassay (FZLIA) to detect HIV infection [130]. The linear dose detection was found in the range of 25–1000 pg/mL. Zinc oxide nanosheet was introduced to detect volatile organic compounds (VOCs) in lung cancer-related diagnosis [131]. The chemiresistive device based on the ZnO could detect diethyl ketone (LOD =0.9 ppb), isopropanol (LOD =11 ppb), acetone (LOD =4 ppb) and other alcohols that indicate lung cancer. Ultrasensitive fluorescent nanoporous ZnO nanoplatform coupled with polyvalent directed peptide was developed for detection of Amyloid-beta 42 ($A\beta_{42}$) as Alzheimer's disease biomarker [132]. It was discovered that by attaching PDPP to the surface of ZnO, the LOD in order to $A\beta_{42}$ rose to 12 ag/ mL compared to the LOD of the commonly used antibody-based method, which is 100 pg mL^{-1}. This ultrasensitive biosensor can support the detection of $A\beta_{42}$ with a 10^4 -times greater LOD compare to the current diagnostic system in order to AD diagnosis.

Nanoflowers shaped ZnO have greater surface area compared to different structures of nano-sized zinc oxides, which is proper for the development of biosensors to detect β-amyloids as the hallmark of neurodegenerative diseases, including insulin-dependent type II diabetes and Alzheimer's disease. ZnO nanoflowers-based sensor was developed and utilized for the detection of amyloids [133]. They enhanced the fluorescence of Thioflavin T (ThT) bonded to the model insulin amyloid bound insulin by absorbing on the ZnO nanoflowers by acting as a reflecting mirror in Fabry-Perot Resonator. Zinc oxide nanorod was also used as an ultrasensitive detector for biosensing of the interleukins, tumor necrosis factor-α as well as biomaerkers, which more examples are provided in Supporting Information.

4.4. TiO_2-based nanoparticles

Titanium dioxide (TiO_2) is a semiconductor NP that is broadly employed in diagnostic and therapeutic uses according to its non-toxicity [134]. TiO_2 NPs, showing good characteristics including high electrical conductivity and high catalytic activity, are one of the extensively applied metal oxides for sensing applications [135,136].

The incorporation of natural organic compounds with TiO_2 NPs can provide high effective detection in the *in vivo* studies. In a study, curcumin was incorporated into TiO_2 NPs and conjugated with the MCP-1 antibody. In fact, the adsorption of curcumin on the surface of TiO_2 NPs occurred efficiently and nanoplatform with a size of about 30 nm was obtained. MCP-1 is greatly expressed in macrophage- areas of atherosclerotic lesions. For the antibody conjugation, the curcumin incorporated titanium dioxide NPs (CTNPs) modified by EDC and NHS were repositioned in the MCP-1 antibody. The MRI scan was performed after the vein injection of CTNPs-MCP-1. Thus, investigations show that these nanoplatforms are a non-toxic, low-cost contrasting agent in order to a non-invasive technique of early detection of atherosclerosis [137]. Table 2 shows various studies in which different metal oxide NPs are applied in early detection of diseases.

5. Metal-organic frameworks (MOFs)

Metal-Organic Frameworks (MOFs) are promise structures that are greatly well-ordered and porous. They grow in a crystal form and are exceptionally flexible, particularly when combined with nanomaterials to the functionality or attributes [143]. They have exclusive properties, such as tunable pore scales, large surface areas, and high adsorption abilities [144]. MOFs have been used as sensitive materials to probes, such as antibodies and aptamers, to form biosensors, such as EC biosensor [144]. Compared with EC biosensors based on common materials such as graphene oxides, those based on MOFs often display high sensitivity for early diagnosis of cancer biomarkers and different diseases. Thus, constructing MOFs-based EC biosensors to identify cancer biomarkers, which are generally very low in tumor issues, is a valuable attempt.

Some binding interactions among MOFs and probes to identify biomarkers include Zr-MOFs-based biosensors made by Zr–O–P bonds to immobilizing probes, such as 509-MOF and UiO-66-NH_2. For example, Zr-MOFs can create Zr–O–P bonds among Zr(IV) clusters. A 509-MOF@aptamer biosensor was established through the creation of varied functional groups. This EC aptasensor was applied to the early diagnosis of different targets based on the changes among the aptamer and targets. The 509-MOF@aptamer -based aptasensor exhibited great stability and high repeatability, which provided a novel sensing assay based on MOFs that could be used for early diagnosis of biomarkers [145]. UiO-66 was modified through FA by coordinative interactions and discovered as a scaffold to an EC cytosensor for living cancer cell detection. FA was bound to folate receptors (FAR), expressed in various cancer cells. The FA@UiO-66-based biosensor showed a LOD of 90 cells/mL and great sensitivity to detect FAR-rich cancer cells [146]. Researchers fabricated an aptasensor based on self-polymerized dopamine-decorated Au and Fe-MOF and then applied it as a biosensing system to CEA detection. Meanwhile, MOF comprises carboxyl groups and Fe^{3+} sites, and NH_2-functionalized CEA aptamer could be attached to it by covalent bonds among amino and carboxyl groups. The aptasensor showed a LOD of 0.33 fg/mL for CEA detection in the range of 1 fg/mL. Though polymers can increase the sensing capability of MOFs-based biosensors, their available synthesis assays are limited [147].

Most EC biosensors based on MOFs have been established to analyze single targets rather than multiple analytes. Although several biomarkers are involved in a disease simultaneously, there is a need to develop multifunctional biosensors. Researchers developed an EC biosensor based on nucleic acid-functionalized MOF for the simultaneous detection of let-7a and miRNA-21 (Fig. 8A). The MOFs were formed using UIO-66-NH_2 to load dyes and dsDNA as a gatekeeper through the nucleic acid hybridization. Two modified MOFs (MB@UIO and TMB@UIO) loaded with electroactive dyes, which covered with dsDNA (dsDNAcapped MOFs) through hybridization of nucleic acid, have been used in the analysis of let-7a and miRNA-21 with LODs of 3.6 and 8 fM, which owner than those of described approaches that focused on single miRNA diagnosis [148].

In another study, a greener-mission Zr(IV)-MOF (BUT-88) was made from a luminescent carbazolyl ligand [149]. BUT-88 shows the first type of MOF with rich linking sites, high biocompatibility and good water stability. BUT-88 was then made into a MOF-based fluorescent nanoprobe (drDNABUT-88 probe), which could detect dual tumor biomarkers, such as miRNA-21 and MUC-1 in MCF-7 cell lines (Fig. 8 C and D). The probe offered improved detection precision in early cancer diagnosis, having a limit of detection (LOD) of 0.13 and 4.50 nM for miRNA-21 and MUC-1, respectively. The obtained LOD of miRNA-21 is lower than those with other sensing methods [150,151].

Recently, near-infrared (NIR) PersL NPs (PLNPs) can act as optical probes bioimaging systems with majorities of low irradiation injury and deep tissue penetration [152]. A chromium (Cr)-doped zinc gallogermanate (ZGGO) @ZIF-8-DOX, with PLNPs as a core and ZIF-8 as a shell to NIR PersL imaging, had been developed. Here, most significantly, the PL phenomenon in ZGGO NP was recognized as the $^2E \rightarrow {}^4A_2$ transition of Cr^{3+}. This platform has a higher resolution than other methods. The mixture of PLNPs and MOF can provide a new imaging method for optical imaging systems. Also, compared to the earlier fluorescent reagent doping, the optical imaging of doping with the non-fluorescent compound is mostly based on the near-infrared (NIR) illumination mechanism [153].

6. Composite and hybrid nanosystems

Different nanomaterials in composite and hybrid systems have been shown to improve biosensor sensitivity. Furthermore, various metals in a nanoformulation enhance the number of reaction sites, resulting in higher reactions and lower LOD [154]. Several structures of nanomaterials have also been used in nanoformulation for the increment of the capability of the biosensor in the detection

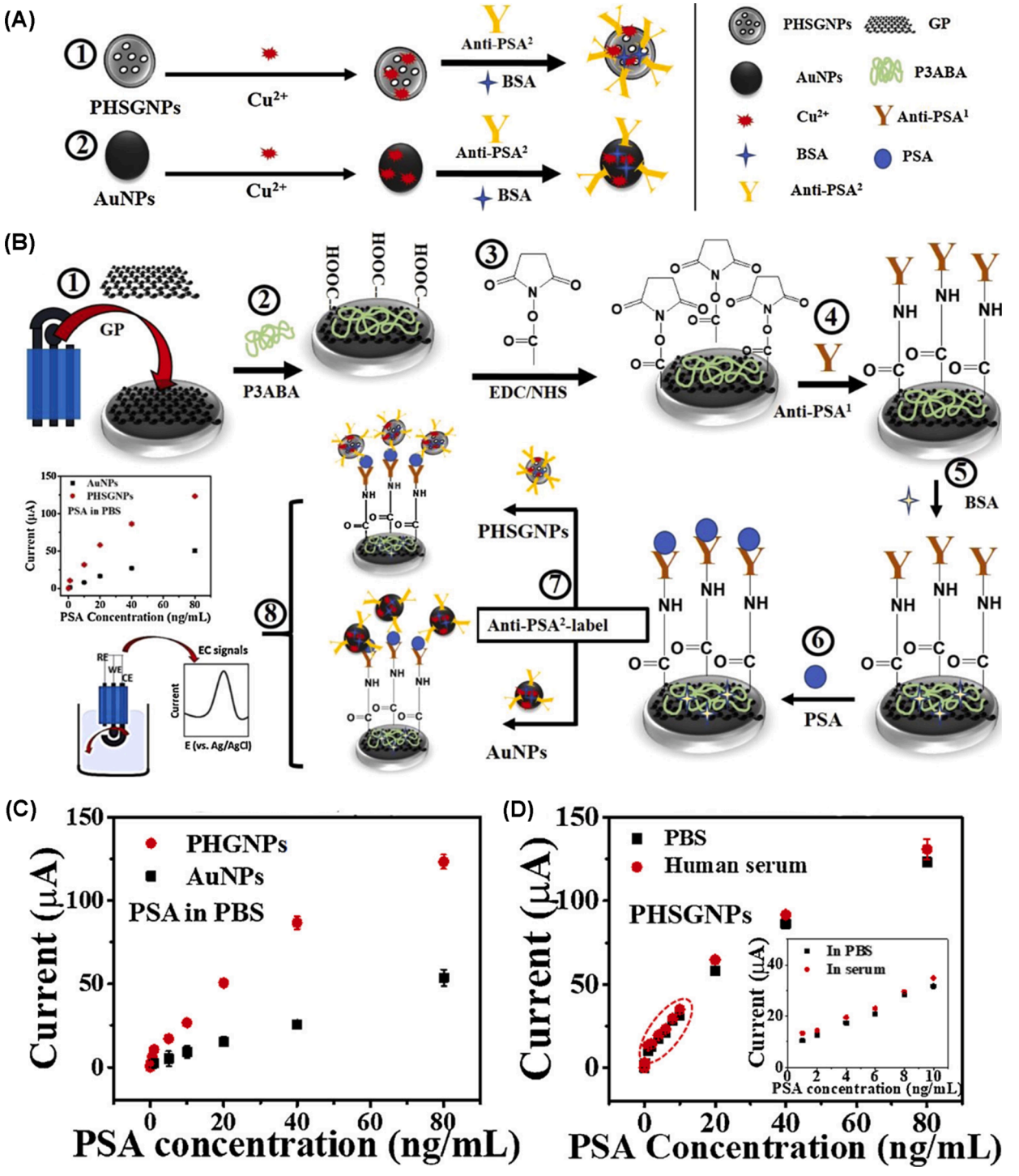

Fig. 9. (**A**) A schematic illustration of the Cu^{2+}-PHSGNPs anti-PSA and Cu^{2+}-AuNPs-anti-PSA. Preparations (**B**) Immunosensor preparation with 8 steps (**C**) The responses from three immunosensors immobilized with PHSGNP and AuNP labelling structures and comparison them. (**D**) Comparison of various pulse voltammetry responses from PHSGNP modified sensors after PSA were spiked in human serum and PBS. Reprinted with permission of Elsevier from Ref [159]. Abbreviations: PHSGNP: Porous-hollowed-silver-gold core-shell NPs. PSA: Prostate specific antigen. PBS: Phosphate-buffered saline.

of biomarkers. Hence, as reported in Table 3, many researchers utilized various composite and hybrid nanosystems for the early detection of diseases.

Nanomaterial-conductive polymer composite based on graphene-poly(3-aminobenzoic acid) (GP-P3ABA) was applied for modification of electrode and Cu ion was also loaded on porous-hollowed-Ag–Au core-shell NPs (PHSGNPs) for signal amplification (Fig. 9 (A and B)) [159]. It was found that utilization of GP-P3ABA modified electrodes resulted in 16 times higher sensing response of prostate specific antigen (PSA) compared to the ones without nanocomposite because of decrement of electrode impedance and higher probe binding sites, respectively. Because Cu ions attached PHSGNPs have a greater surface area than AuNPs, the created system demonstrated a threefold increase in electrochemical current from PHSGNPs. GP-P3ABA modified electrode with PHSGNP labeling improved sensing performance by 120 times compared to AuNP labeling (Fig. 9 (C and D)). The system's LOD was 0.1 pg/mL, four orders of magnitude more than the clinically related value in human serum.

Au@Ag core-shell NPs/graphene quantum dots (Au@Ag/GQDs) composite was synthesized and applied for preparation of highly sensitive electrochemiluminescent (ECL) sensor as a signal indicator to identify greatly up-regulated liver cancer (HULC) [172]. It was indicated that the Au@Ag NPs showed large surface area, and higher electronic transmission capacity because of the synergistic effect of Au and Ag in the core-shell structure. The ECL sensor also displayed superior sensitivity for the diagnosis of HULC with a LOD of 0.3 fM in optimal conditions.

Magnetic-beads (MBs)-based aptamers/metal NPs based on AuNPs and AgNPs were used in the preparation of inductively coupled plasma mass spectrometry (ICP-MS) in order to detection of lung carcinoma cell (A549) and hepatocellular carcinoma cell (SMMC-7721) [173]. It was exhibited that the DNA hybridization chain reaction happened simultaneously, counting A549 and SMMC-7721 cells. It was indicated that the suggested assay could be used in order to simultaneous detection of the low amount of cancer cells, including 50 SMMC-7721 and A549 cells in serum during 1 h with a recovery of 93−108%.

An affordable biosensor was created by isotype ZnO/CdO heterostructure for sensing acetone which in human breath shows the onset of different diseases [174]. The ZnO/CdO heterostructure indicated a selective photoresponse of 540 with response times of 61s, respectively, to 1 ppm of acetone vapour. Under photo-activating with LED light, the formation of photogenerated electrons and holes on the surface of ZnO/CdO heterostructure led to the enhancement of carrier concentration and reduction of the potential barrier height. Therefore, as it is shown, more electrons can be transferred to the conduction band of ZnO, increasing the adsorption sites of the ZnO/CdO heterostructure. The prepared sensor exhibited a LOD of 1 ppm with high stability. More examples are provided in Supporting Information.

7. Technology-based advanced metal biosensors

Despite advances in metal-based biosensors, one of the challenges is early detection at low concentrations**.** The integration of metal-based optical and electrochemical nanoosensor with other technologies such as microfluidic devices, smartphones, and implantable device can be applied to improve the potential of sensing devices in the early detection of diseases [175,176].

7.1. Microfluidic-based metal biosensor

The microfluidic biosensors are robust systems that provide high-throughput techniques and quick real-time detection in addition to increased analytical performance [177,178]. In the 1990s, this technology was advanced as a small-scale technology typically made up of microchannels and microdomains ranging in size from tens to hundreds of micrometers [179]. Metal biosensor-based microfluidics can overcome some of the limitations of common biosensors. Some of these limitations are listed in Table 4. Generally, the microfluidic technique controls liquid at the microscale; even smaller volumes [175].

Various ZnO nanowires with different diameter and length were prepared through the hydrothermal growth in microfluidic channels by varying the amount of PEI [180]. It was indicated that by increasing the growth and the content of PEI to 3 h and 5.0 mM the optimized average diameter and length of ZnO nanowire reached to 0.1 μm and 8.7 μm, respectively. The optimal ZnO nanowire resulted in superior LOD of 1 pg/mL in order to human α-fetoprotein assay and 100 fg/mL in order to carcinoembryonic antigen assay.

Interdigitated microelectrodes with microfluidic shows a diagnosis with the high sensitivity. Wang et al. developed multifunctional microfluidic chip with a Tesla detection zone, mixing zone, and microelectrodes to improve the sensitivity of

Table 4
Comparison between novel technologies-based biosensors and conventional diagnostic biosensors.

Biosensors	Benefits	Limitations
Current metal-based biosensors	ü Relatively basic setup ü Wide utilization in	ü Less sensitivity ü Low reproducibility ü Requires high volume
Microfluidic-based metal biosensors	ü Decreased sample volumes ü Enhanced speed ü Increased sensitivity, ü Ease of multisample analysis	ü Channel clogging ü Cost of synthesis
Smartphone-based metal biosensors	ü provides fast and accurate analysis ü provides cost-effective diagnostics of multiple analytes	ü Sensitive to the change of ambient conditions ü Cost of measurement circuitry

impedimetric diagnosis of Escherichia coli through Ag NPs to increase impedance signals, and a sensitivity of 500 CFU/mL was established. Here, bacteria was coated with polymer diallyldimethylammonium chloride (PDDA), and when AuNPs are added, the *E. coli* / PDDA / AuNPs set is formed. The surface of bacteria is negatively charged. However, there is a great amount of ammonium cationic in PDDA solution. *E.coli*/PDDA complexes can be made by static adsorption among the negatively charged bacteria and the positively charged PDDA. When AuNPs and *E. coli*/PDDA complexes were simultaneously injected into the mixing zone of the chip, the complexes formed according to electrostatic contact. Then, the complexes were taken on the edge of microelectrodes through reduction of Ag ions on the surface of AuNP. When adding Ag NPs, the complex is enriched in the edge of microelectrodes inside the detection zone [172].

7.2. Smartphone-based metal biosensors

The smartphone can benefit from the latest developments in nanotechnology in order to develop diagnostic methods [181]. The integration of smartphone systems with the metal-based biosensor is actually a leaving from the traditional biosensing devices, proposing transportable health care diagnostics outside laboratories [182]. In reality, smartphone-based biosensors are more affordable and accessible than conventional devices, making them an affordable option for real-time and POC sensing [183]. Smartphone-based biosensors have been developed by various methods. In an ideal biosensor, the biosensing process is integrated with a detector (smartphone), resulting in an independent biosensor [184,185].

Various colourimetric and optical technique incorporation can be applied to convert the smartphone into a laboratory device to perform different analytical analyses. In a study, Hsu et al. proposed a POC test containing a nanozyme platinum and Pt@Au NPs as a signal probe, immunosensor, and smartphone, which could be applied to precise diagnosis of Zikv viruse in whole blood. Fig. 10A shows the steps of a VISZIKV fabrication as follows; first deposition of polyethylenimine (bPEI) on a rich amine-functionalized chip occurred, and AbZIKV was conjugated on the bPEI-based chips through a functional crosslinker that consists of N-hydroxysuccinimide ester, permitting covalent binding of amine groups on the chips with the sulfhydryl groups on thiolated AbZIKV. The chip was connected on the vial, which can be applied to capture virus (Fig. 10B). This technology is capable to detect the virus with a great sensitivity of 1 pg/mL. The POC test is made on whole blood without any need of filtration, and the expriment can be simply worked through calculation using a smartphone [186].

Researcher also developed a ZNO nanorods microfluidics chip -based smartphone for cheap and rapid sensitive colorimetric detection of viral in short times. The channels of these nanoplatform are made of ZnO nanorods structures, which can improve the capture of the virus and the sensitivity of detection. Here, after the connection of antibodies to the microchannel surface, the AuNPs-

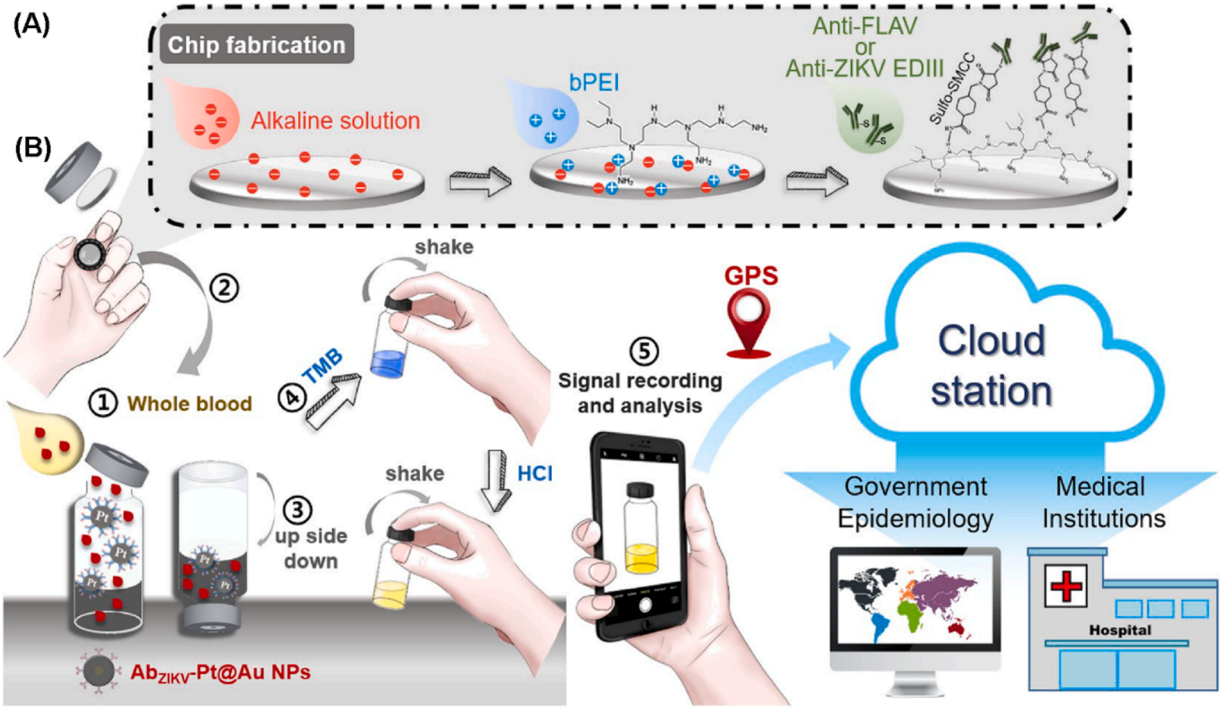

Fig. 10. (**A**) Schematic of VIS$_{ZIKV}$ fabrication; (**B**) Schematic shows the processes of detection, 1. Blood sample added to the VIS$_{ZIKV}$; 2. Securing of chips containing lid; 3. Shaking, incubating, and transferring the lid to a vial comprising wash buffer; 4. moving the lid to a novel vial comprising H2O2/TMB, 5. recording of signal through a smartphone. This platform containing a VIS$_{ZIKV}$, Ab$_{ZIKV}$-Pt@Au NPs, and a smartphone in order to quick detection of ZIKV in whole blood. This system facilitates data storage Reprinted with permission of Elsevier from Ref [186]. Abbreviations: ZIKV: Zika virus. Pt@Au NPs: Platinum/gold core-shell NPs.

antibodies attaches to the virus. Silver is used in this platform to extend the detection limit and function as a signal amplifier. The sensitivity of this nanoplatform was attained about 2.7 × 10^4 EID50/ml [187]. These POC microfluidic system integrated with smartphone would offer high sensitivity, cheap and fast nanoplatform for detection of virus in low-concentration. More examples are provided in Supporting Information.

8. Conclusion and future perspective

This review provides a summary of current advancements in the use of metal NPs in the early diagnosis of diseases. Recently, many researchers have tried to develop early diagnosis of diseases using metal NPs. Metal NP-based technologies provide more selectivity and sensitivity compared to the present instruments for early illness detection accessible in the clinic, or they provide whole new capabilities that are not possible with conventional techniques. Although the selectivity and sensitivity of biomarker detection is improving, the laboratory diagnostic is not adaptable with clinical practice.

The unique and tunable optical properties of metal NPs have revealed high potential in the expansion of biosensing and bioimaging techniques. Among all metallic NPs, gold and silver NPs show the most exciting physical properties for biosensing. The great sensitivity and non-invasiveness of AuNP-based optical biosensors make them particularly suitable for use as POC devices. In fact, AgNPs have drawn a lot of attention as very sensitive materials for plasmonic biosensors. Although AgNPs are less stable and biocompatible than AuNPs, they nonetheless provide highly sensitive plasmonic biosensors for early diagnoses, particularly for pandemic illnesses like COVID-19. Furthermore, the use of Au with Ag NPs in core@shell structures offers a protective shell, and improves the plasmonic response of the resulting colloids. Some metal NPs such as CdS and Pd NPs with catalytic and photocatalytic activity are suitable candidates for early detection of contaminants, H_2O_2 and biomarkers. A high sensitivity in early detection could well be attained through using metal oxide NPs because of their huge surface area, quick electron transfer kinetics, biocompatibility, and catalytic activity. This potential has prompted the application of metal oxide NPs in the development of several biosensors for pathogens, biological molecules, and biomarkers. The created nanocomposite and nanohybride-based biosensors can offer fresh approaches to difficult analytical evaluation and detection problems. Moreover, the exclusive properties of nanocomposites with improved sensitivity and stability make them suitable for early diagnosis methods and real-time sensing in complex matrices. MOFs have porous structures with high surface areas, therefore composites containing MOFs with functional materials have been applied in biosensor uses. Additionally, the MOFs have beneficial fluorescence quenching capability to fluorescence-labelled DNA probes.

However, there are some limitations to the performance of metal-based biosensors, including controlling their morphology based on the formation method, mass production of biosensors for disease and virus detection, toxicity and biocompatibility [188,189]. By overcoming these limitations, some technologies can improve the performance of biosensors and diagnostic sensitivity. The

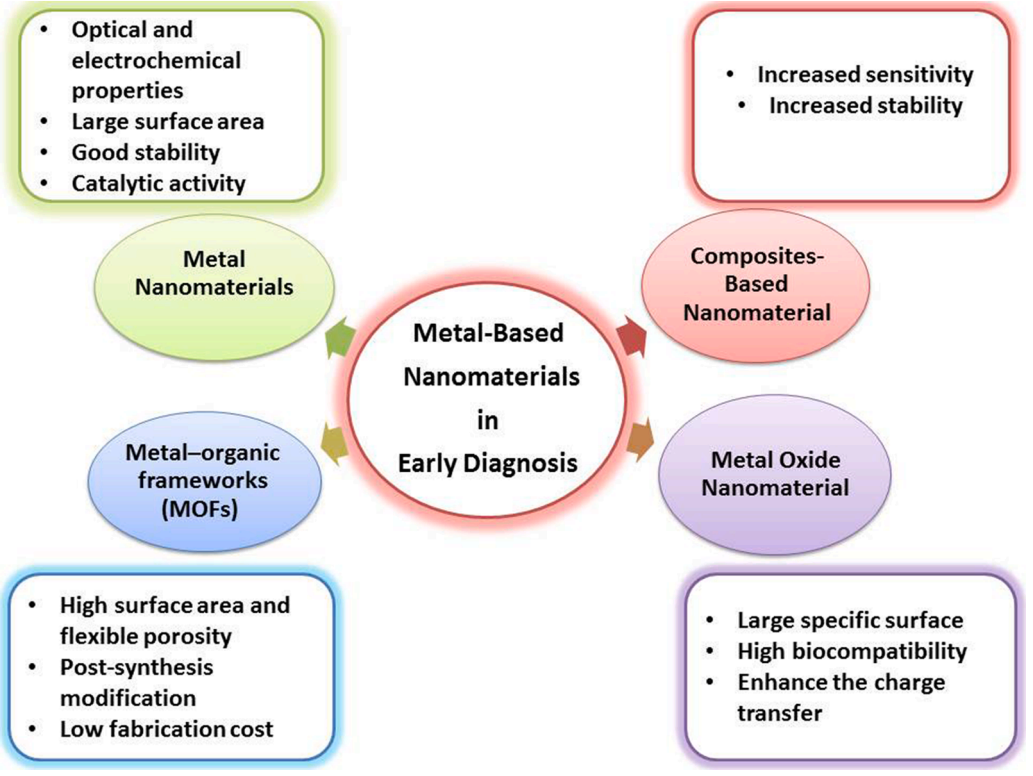

Fig. 11. Several metal-based nanomaterials' favorable characteristics for early diagnosis.

combination of microfluidics and biosensor provides the following advantages: sophisticated assays for flow-based detection and improved signal-to-noise ratios. However, the shear impact of microfluidic flow on the immobilized antibodies in the biosensing platform also has certain limitations. In order to use metals and metal oxide, NPs in the development of biosensors for the early identification of diseases, several essential features of these materials have been mentioned in Fig. 11.

To accelerate the clinical application of metal NP-based early diagnosis methods many challenges need to be addressed:

1. Producing a large-scale nanoprobe with great sensitivity, affordable high reproducibility and stability is still a major limitation; as a result, to reduce these changes, it is necessary to simplify the synthesis of nanoprobes.
2. Metal NP-based detection signals can be affected by many parameters such as nonspecific connection of NP probes, improper detection conditions and aggregation of NPs. The complex composition of body fluids may cause signal fluctuations, which can have an impact on the dependability and repeatability of detection outcomes.
3. The size, shape, surface chemistry, charge, and targeted ligands of NPs affect their toxicity. To avoid the toxicity of metal NPs and to help conserve energy, green synthesis techniques can be used to create non-toxic NPs from natural sources including microorganisms and plant extracts. The use of comprehensive NPs' physiochemical characteristics, diverse biological matrix research, and their implications for the bioavailability and toxicity of living organisms in investigations can also help solve this issue. In general, all sectors, notably academic researchers, industry engineers, clinical specialists, and governments, should collaborate to bring this nanotechnology into the clinic for the early diagnosis of illnesses in the near future.

CRediT authorship contribution statement

Maryam Jouyandeh: Writing – review & editing, Validation. **S. Mohammad Sajadi:** Writing – review & editing. **Farzad Seidi:** Writing – review & editing, Visualization. **Sajjad Habibzadeh:** Writing – review & editing. **Muhammad Tajammal Munir:** Writing – review & editing. **Otman Abida:** Formal analysis. **Sepideh Ahmadi:** Writing – review & editing, Conceptualization. **Daria Kowalkowska-Zedler:** Investigation. **Navid Rabiee:** Writing – review & editing, Conceptualization, Supervision. **Mohammad Rabiee:** Writing – review & editing, Conceptualization. **Golnaz Heidari:** Writing – review & editing. **Mahnaz Hassanpour:** Visualization, Writing – review & editing. **Ehsan Nazarzadeh Zare:** Writing – review & editing, Visualization. **Mohammad Reza Saeb:** Writing – review & editing, Conceptualization, Supervision.

Declaration of interests

The authors declare that they have no known competing financial interests or personal relationships that could have appeared to influence the work reported in this paper.

Supplementary materials

Supplementary material associated with this article can be found, in the online version, at doi:10.1016/j.onano.2022.100104.

References

[1] N. Rabiee, M. Bagherzadeh, M. Heidarian Haris, A.M. Ghadiri, F. Matloubi Moghaddam, Y. Fatahi, R. Dinarvand, A. Jarahiyan, S. Ahmadi, M. Shokouhimehr, Polymer-Coated NH2-UiO-66 for the Codelivery of DOX/pCRISPR, ACS Appl. Mater. Interfaces 13 (2021) 10796–10811.
[2] S. Ahmadi, N. Rabiee, Y. Fatahi, S.E. Hooshmand, M. Bagherzadeh, M. Rabiee, V. Jajarmi, R. Dinarvand, S. Habibzadeh, M.R. Saeb, Green chemistry and coronavirus, Sustain. Chem. Pharmacy (2021), 100415.
[3] G.B. Frisoni, M. Boccardi, F. Barkhof, K. Blennow, S. Cappa, K. Chiotis, J.-F. Démonet, V. Garibotto, P. Giannakopoulos, A. Gietl, Strategic roadmap for an early diagnosis of Alzheimer's disease based on biomarkers, Lancet Neurol. 16 (2017) 661–676.
[4] L.A.L. Tang, J. Wang, K.P. Loh, Graphene-based SELDI probe with ultrahigh extraction and sensitivity for DNA oligomer, J. Am. Chem. Soc. 132 (2010) 10976–10977.
[5] E. Hashemi, O. Akhavan, M. Shamsara, S. Valimehr, R. Rahighi, DNA and RNA extractions from eukaryotic and prokaryotic cells by graphene nanoplatelets, RSC Adv. 4 (2014) 60720–60728.
[6] S.J. Heerema, C. Dekker, Graphene nanodevices for DNA sequencing, Nat. Nanotechnol. 11 (2016) 127–136.
[7] N. Rabiee, S. Ahmadi, R. Afshari, S. Khalaji, M. Rabiee, M. Bagherzadeh, Y. Fatahi, R. Dinarvand, M. Tahriri, L. Tayebi, Polymeric nanoparticles for nasal drug delivery to the brain: relevance to Alzheimer's disease, Adv. Therap. 4 (2021), 2000076.
[8] S.F. Parsa, A. Vafajoo, A. Rostami, R. Salarian, M. Rabiee, N. Rabiee, G. Rabiee, M. Tahriri, A. Yadegari, D. Vashaee, Early diagnosis of disease using microbead array technology: a review, Anal. Chim. Acta 1032 (2018) 1–17.
[9] W. Lin, Introduction: nanoparticles in medicine, Chem. Rev. 115 (2015) 10407–10409.
[10] L.R. Hirsch, R.J. Stafford, J. Bankson, S.R. Sershen, B. Rivera, R. Price, J.D. Hazle, N.J. Halas, J.L. West, Nanoshell-mediated near-infrared thermal therapy of tumors under magnetic resonance guidance, Proc. Natl. Acad. Sci. U. S. A. 100 (2003) 13549–13554.
[11] S. Ahmadi, N. Rabiee, M. Bagherzadeh, F. Elmi, Y. Fatahi, F. Farjadian, N. Baheiraei, B. Nasseri, M. Rabiee, N.T. Dastjerd, A. Valibeik, M. Karimi, M. R. Hamblin, Stimulus-responsive sequential release systems for drug and gene delivery, Nano Today 34 (2020), 100914.
[12] N. Rabiee, M. Bagherzadeh, M. Kiani, A.M. Ghadiri, Rosmarinus officinalis directed palladium nanoparticle synthesis: investigation of potential anti-bacterial, anti-fungal and Mizoroki-Heck catalytic activities, Adv. Powder Technol. 31 (2020) 1402–1411.
[13] A. Assali, O. Akhavan, M. Adeli, S. Razzazan, R. Dinarvand, S. Zanganeh, M. Soleimani, M. Dinarvand, F. Atyabi, Multifunctional core-shell nanoplatforms (gold@ graphene oxide) with mediated NIR thermal therapy to promote miRNA delivery, Nanomed.: Nanotechnol., Biol. Med. 14 (2018) 1891–1903.

[14] N. Rabiee, M. Bagherzadeh, A. Ghasemi, H. Zare, S. Ahmadi, Y. Fatahi, R. Dinarvand, M. Rabiee, S. Ramakrishna, M. Shokouhimehr, R.S. Varma, Point-of-use rapid detection of SARS-CoV-2: nanotechnology-enabled solutions for the COVID-19 pandemic, Int. J. Mol. Sci. 21 (2020).
[15] S. Ahmadi, H. Kamaladini, F. Haddadi, M.R. Sharifmoghadam, Thiol-capped gold nanoparticle biosensors for rapid and sensitive visual colorimetric detection of klebsiella pneumoniae, J. Fluorescence 28 (2018) 987–998.
[16] F. Dabbagh Moghaddam, F. Romana Bertani, Application of Microfluidic Platforms in Cancer Therapy, Mater. Chem. Horizons 1 (1) (2022) 69–88.
[17] M.K. Yazdi, P. Zarrintaj, B. Bagheri, Y.C. Kim, M.R. Ganjali, M.R. Saeb, 32 - Nanotechnology-based biosensors in drug delivery, Ed., in: M. Mozafari (Ed.), Nanoengineered Biomaterials for Advanced Drug Delivery, Elsevier, 2020, pp. 767–779.
[18] A. Mehdizadeh, P. Najafi Moghadam, S. Ehsanimehr, A. Fareghi, Preparation of a new magnetic nanocomposite for the removal of dye pollutions from aqueous solutions: synthesis and characterization, Mater. Chem. Horizons 1 (1) (2022) 23–34.
[19] C.D. Medley, J.E. Smith, Z. Tang, Y. Wu, S. Bamrungsap, W. Tan, Gold nanoparticle-based colorimetric assay for the direct detection of cancerous cells, Anal Chem. 80 (2008) 1067–1072.
[20] N. Movagharnezhad, S. Ehsanimehr, P. Najafi Moghadam, Synthesis of Poly (N-vinylpyrrolidone)-grafted-Magnetite Bromoacetylated Cellulose via ATRP for Drug Delivery, Mater. Chem. Horizons 1 (2) (2022) 89–98.
[21] T.A. Rocha-Santos, Sensors and biosensors based on magnetic nanoparticles, Trends Analyt. Chem. 62 (2014) 28–36.
[22] R. Ghanbari, D. Khorsandi, A. Zarepour, M. Ghomi, A. Fahimipour, Z. Tavakkoliamol, A. Zarrabi, Ionic Liquid-based Sensors, Mater. Chem. Horizons 1 (2) (2022) 123–135.
[23] N. Rabiee, M. Bagherzadeh, A.M. Ghadiri, G. Salehi, Y. Fatahi, R. Dinarvand, ZnAl nano layered double hydroxides for dual functional CRISPR/Cas9 delivery and enhanced green fluorescence protein biosensor, Sci. Rep. 10 (2020) 1–15.
[24] A. Lyberopoulou, E.P. Efstathopoulos, M. Gazouli, Nanotechnology-based rapid diagnostic tests. Proof and Concepts in Rapid Diagnostic Tests and Technologies, IntechOpen, 2016, pp. 89–105.
[25] B. Nasseri, M. Turk, K. Kosemehmetoglu, M. Kaya, E. Piskin, N. Rabiee, T.J. Webster, The pimpled gold nanosphere: a superior candidate for plasmonic photothermal therapy, Int. J. Nanomed. 15 (2020) 2903.
[26] P.R. Solanki, A. Kaushik, V.V. Agrawal, B.D. Malhotra, Nanostructured metal oxide-based biosensors, NPG Asia Mater. 3 (2011) 17–24.
[27] X. Luo, A. Morrin, A.J. Killard, M.R. Smyth, Application of nanoparticles in electrochemical sensors and biosensors, Electroanal.: Int. J. Devot. Fundam. Pract. Aspects Electroanal. 18 (2006) 319–326.
[28] M. Shobana, Nanoferrites in biosensors–a review, Mater. Sci. Eng.: B 272 (2021), 115344.
[29] M.J. Hajipour, O. Akhavan, A. Meidanchi, S. Laurent, M. Mahmoudi, Hyperthermia-induced protein corona improves the therapeutic effects of zinc ferrite spinel-graphene sheets against cancer, RSC Adv. 4 (2014) 62557–62565.
[30] M. Nodehi, A. Kiasadr, G. Babaee Bachevanlo, Modified glassy carbon electrode with mesoporous Silica-Metformin/Multi-Walled carbon nanotubes as a biosensor for ethinylestradiol detection, Mater. Chem. Horizons (2022), https://doi.org/10.22128/mch.2022.601.1024. In press.
[31] S. Ramanathan, S.C. Gopinath, M.M. Arshad, P. Poopalan, P. Anbu, A DNA based visual and colorimetric aggregation assay for the early growth factor receptor (EGFR) mutation by using unmodified gold nanoparticles, Mikrochim. Acta 186 (2019) 1–13.
[32] N. Rabiee, M. Bagherzadeh, A.M. Ghadiri, Y. Fatahi, A. Aldhaher, P. Makvandi, R. Dinarvand, M. Jouyandeh, M.R. Saeb, M. Mozafari, Turning toxic nanomaterials into a safe and bioactive nanocarrier for co-delivery of DOX/pCRISPR, ACS Appl. Bio Materi. 4 (2021) 5336–5351.
[33] A. Camarca, A. Varriale, A. Capo, A. Pennacchio, A. Calabrese, C. Giannattasio, C. Murillo Almuzara, S. D'Auria, M. Staiano, Emergent biosensing technologies based on fluorescence spectroscopy and surface plasmon resonance, Sensors 21 (2021) 906.
[34] A.B. Taylor, P. Zijlstra, Single-molecule plasmon sensing: current status and future prospects, ACS Sens. 2 (2017) 1103–1122.
[35] S. Ahmadi, N. Rabiee, M. Bagherzadeh, M. Karimi, Chapter 6 - Microfluidic devices for pathogen detection, Eds., in: M.R. Hamblin, M. Karimi (Eds.), Biomedical Applications of Microfluidic Devices, Academic Press, 2021, pp. 117–151.
[36] N. Baig, I. Kammakakam, W. Falath, Nanomaterials: a review of synthesis methods, properties, recent progress, and challenges, Mater. Adv. 2 (2021) 1821–1871.
[37] A. Rahman, M.A. Chowdhury, N. Hossain, Green synthesis of hybrid nanoparticles for biomedical applications: a review, Appl. Surf. Sci. Adv. 11 (2022), 100296.
[38] K.B. Narayanan, N. Sakthivel, Phytosynthesis of gold nanoparticles using leaf extract of Coleus amboinicus Lour, Mater. Character. 61 (2010) 1232–1238.
[39] S. Iravani, H. Korbekandi, S.V. Mirmohammadi, B. Zolfaghari, Synthesis of silver nanoparticles: chemical, physical and biological methods, Res. Pharm. Sci. 9 (2014) 385–406.
[40] I. Ijaz, E. Gilani, A. Nazir, A. Bukhari, Detail review on chemical, physical and green synthesis, classification, characterizations and applications of nanoparticles, Green Chem. Lett. Rev. 13 (2020) 223–245.
[41] D. Zhang, X.-l. Ma, Y. Gu, H. Huang, G.-w. Zhang, Green synthesis of metallic nanoparticles and their potential applications to treat cancer, Front. Chem. 8 (2020).
[42] S.V. Banne, M.S. Patil, R.M. Kulkarni, S.J. Patil, Synthesis and characterization of silver nano particles for EDM applications, Mater. Today Proc. 4 (2017) 12054–12060.
[43] M. Doble, K. Rollins, A. Kumar, Green Chemistry and Engineering, Academic Press, 2010.
[44] D. Nath, P. Banerjee, Green nanotechnology – a new hope for medical biology, Environ. Toxicol. Pharmacol. 36 (2013) 997–1014.
[45] V. Gokila, V. Perarasu, R. Rufina, Qualitative comparison of chemical and green synthesized Fe3O4 nanoparticles, Adv. Nano Res. 10 (2021) 71–76.
[46] O. Pashchenko, T. Shelby, T. Banerjee, S. Santra, A comparison of optical, electrochemical, magnetic, and colorimetric point-of-care biosensors for infectious disease diagnosis, ACS Infect. Dis. 4 (2018) 1162–1178.
[47] D.D. Gurav, Y.A. Jia, J. Ye, K. Qian, Design of plasmonic nanomaterials for diagnostic spectrometry, Nanosc. Adv. 1 (2019) 459–469.
[48] M.R. Jones, K.D. Osberg, R.J. Macfarlane, M.R. Langille, C.A. Mirkin, Templated techniques for the synthesis and assembly of plasmonic nanostructures, Chem. Rev. 111 (2011) 3736–3827.
[49] B.-Y. Chang, S.-M. Park, Electrochemical impedance spectroscopy, Annu. Rev. Anal. Chem. 3 (2010) 207–229.
[50] O. Tokel, F. Inci, U. Demirci, Advances in plasmonic technologies for point of care applications, Chem. Rev. 114 (2014) 5728–5752.
[51] A.A. Jamal, B. Witzigmann, Plasmonic Perfect Absorbers for Biosensing Applications, Plasmonics 9 (2014) 1265–1270.
[52] X. Wu, Y. Xia, Y. Huang, J. Li, H. Ruan, T. Chen, L. Luo, Z. Shen, A. Wu, Improved SERS-active nanoparticles with various shapes for CTC detection without enrichment process with supersensitivity and high specificity, ACS Appl. Mater. Interfaces 8 (2016) 19928–19938.
[53] C. Song, Y. Yang, B. Yang, L. Min, L. Wang, Combination assay of lung cancer associated serum markers using surface-enhanced Raman spectroscopy, J. Mater. Chem. B 4 (2016) 1811–1817.
[54] S. Dutta Choudhury, R. Badugu, K. Ray, J.R. Lakowicz, Silver–gold nanocomposite substrates for metal-enhanced fluorescence: ensemble and single-molecule spectroscopic studies, J. Phys. Chem. 116 (2012) 5042–5048.
[55] F. Liu, M.M. Wong, S.K. Chiu, H. Lin, J.C. Ho, S.W. Pang, Effects of nanoparticle size and cell type on high sensitivity cell detection using a localized surface plasmon resonance biosensor, Biosens. Bioelectron. 55 (2014) 141–148.
[56] L. Soares, A. Csáki, J. Jatschka, W. Fritzsche, O. Flores, R. Franco, E. Pereira, Localized surface plasmon resonance (LSPR) biosensing using gold nanotriangles: detection of DNA hybridization events at room temperature, Analyst 139 (2014) 4964–4973.
[57] B. Jung, W. Frey, Fabrication and localized surface plasmon properties of triangular gold nanowell arrays in a glass substrate, J. Nanosci. Nanotechnol. 15 (2015) 688–692.
[58] P. Malik, R. Gupta, V. Malik, R.K. Ameta, Emerging nanomaterials for improved biosensing, Meas.: Sens. 16 (2021), 100050.
[59] H. Malekzad, P.S. Zangabad, H. Mirshekari, M. Karimi, M.R. Hamblin, Noble metal nanoparticles in biosensors: recent studies and applications, Nanotechnol. Rev. 6 (2017) 301–329.

[60] K. Alaqad, T.A. Saleh, Gold and silver nanoparticles: synthesis methods, characterization routes and applications towards drugs, J. Environ. Anal. Toxicol. 6 (2016) 525–2161.
[61] G. Heidari, M. Hassanpour, F. Nejaddehbashi, M. Sarfjoo, S. Yousefiasl, E. Sharifi, A. Bigham, T. Agarwal, A. Borzacchiello, E. Lagreca, C. Di Natale, N. Nikfarjam, Y. Vasseghian, Biosynthesized Nanomaterials with Antioxidant and Antimicrobial Properties, Mater. Chem. Horizons 1 (1) (2022) 35–48.
[62] P. Velusamy, C.-H. Su, G. Venkat Kumar, S. Adhikary, K. Pandian, S.C. Gopinath, Y. Chen, P. Anbu, Biopolymers regulate silver nanoparticle under microwave irradiation for effective antibacterial and antibiofilm activities, PLoS One 11 (2016), e0157612.
[63] P. Tan, H. Li, J. Wang, S.C. Gopinath, Silver nanoparticle in biosensor and bioimaging: clinical perspectives, Biotechnol. Appl. Biochem. (2020).
[64] S. Iravani, H. Korbekandi, S.V. Mirmohammadi, B. Zolfaghari, Synthesis of silver nanoparticles: chemical, physical and biological methods, Res. Pharm. Sci. 9 (2014) 385.
[65] A.D. Kurdekar, L.A. Chunduri, S.M. Chelli, M.K. Haleyurgirisetty, E.P. Bulagonda, J. Zheng, I.K. Hewlett, V. Kamisetti, Fluorescent silver nanoparticle based highly sensitive immunoassay for early detection of HIV infection, RSC Adv. 7 (2017) 19863–19877.
[66] M. Jafari, E. Solhi, S. Tagi, M. Hasanzadeh, V. Jouyban-Gharamaleki, A. Jouyban, N. Shadjou, Non-invasive quantification of malondialdehyde biomarker in human exhaled breath condensate using self-assembled organic-inorganic nanohybrid: a new platform for early diagnosis of lung disease, J. Pharm. Biomed. Anal. 164 (2019) 249–257.
[67] G. Lentini, E. Fazio, F. Calabrese, L.M. De Plano, M. Puliafico, D. Franco, M.S. Nicolò, S. Carnazza, S. Trusso, A. Allegra, Phage–AgNPs complex as SERS probe for U937 cell identification, Biosens. Bioelectron. 74 (2015) 398–405.
[68] T. Zheng, N. Pierre-Pierre, X. Yan, Q. Huo, A.J. Almodovar, F. Valerio, I. Rivera-Ramirez, E. Griffith, D.D. Decker, S. Chen, Gold nanoparticle-enabled blood test for early stage cancer detection and risk assessment, ACS Appl. Mater. Interfaces 7 (2015) 6819–6827.
[69] M. Jazayeri, H. Amani, A. Pourfatollah, A. Avan, G. Ferns, H. Pazoki-Toroudi, Enhanced detection sensitivity of prostate-specific antigen via PSA-conjugated gold nanoparticles based on localized surface plasmon resonance: GNP-coated anti-PSA/LSPR as a novel approach for the identification of prostate anomalies, Cancer Gene Ther. 23 (2016) 365–369.
[70] W. Lu, A.K. Singh, S.A. Khan, D. Senapati, H. Yu, P.C. Ray, Gold nano-popcorn-based targeted diagnosis, nanotherapy treatment, and in situ monitoring of photothermal therapy response of prostate cancer cells using surface-enhanced Raman spectroscopy, J. Am. Chem. Soc. 132 (2010) 18103–18114.
[71] K.T. Butterworth, J.R. Nicol, M. Ghita, S. Rosa, P. Chaudhary, C.K. McGarry, H.O. McCarthy, G. Jimenez-Sanchez, R. Bazzi, S. Roux, Preclinical evaluation of gold-DTDTPA nanoparticles as theranostic agents in prostate cancer radiotherapy, Nanomedicine 11 (2016) 2035–2047.
[72] A. Parnsubsakul, R.E. Safitri, P. Rijiravanich, W. Surareungchai, Electrochemical assay of proteolytically active prostate specific antigen based on anodic stripping voltammetry of silver enhanced gold nanoparticle labels, J. Electroanal. Chem. 785 (2017) 125–130.
[73] M. Eghtedari, A.V. Liopo, J.A. Copland, A.A. Oraevsky, M. Motamedi, Engineering of hetero-functional gold nanorods for the in vivo molecular targeting of breast cancer cells, Nano Lett. 9 (2009) 287–291.
[74] J.C.Y. Kah, K.W. Kho, C.G.L. Lee, C.J. Richard, Early diagnosis of oral cancer based on the surface plasmon resonance of gold nanoparticles, Int. J. Nanomed. 2 (2007) 785.
[75] X. Qian, X.-H. Peng, D.O. Ansari, Q. Yin-Goen, G.Z. Chen, D.M. Shin, L. Yang, A.N. Young, M.D. Wang, S. Nie, In vivo tumor targeting and spectroscopic detection with surface-enhanced Raman nanoparticle tags, Nat. Biotechnol. 26 (2008) 83–90.
[76] Z. Altintas, S.S. Kallempudi, Y. Gurbuz, Gold nanoparticle modified capacitive sensor platform for multiple marker detection, Talanta 118 (2014) 270–276.
[77] J.-W. Choi, D.-Y. Kang, Y.-H. Jang, H.-H. Kim, J. Min, B.-K. Oh, Ultra-sensitive surface plasmon resonance based immunosensor for prostate-specific antigen using gold nanoparticle–antibody complex, Colloids Surf. A: Physicochem. Eng. Aspects 313 (2008) 655–659.
[78] J.-H. Lee, D.-Y. Kang, T. Lee, S.-U. Kim, B.-K. Oh, J.-W. Choi, Signal enhancement of surface plasmon resonance based immunosensor using gold nanoparticle–antibody complex for β-Amyloid (1-40) detection, J. Nanosci. Nanotechnol. 9 (2009) 7155–7160.
[79] X. Shi, S. Wang, S. Meshinchi, M.E. Van Antwerp, X. Bi, I. Lee, J.R. Baker Jr, Dendrimer-entrapped gold nanoparticles as a platform for cancer-cell targeting and imaging, Small 3 (2007) 1245–1252.
[80] Q. Zhang, X. Lu, P. Tang, D. Zhang, J. Tian, L. Zhong, Gold nanoparticle (AuNP)-based surface-enhanced Raman scattering (SERS) probe of leukemic lymphocytes, Plasmonics 11 (2016) 1361–1368.
[81] Y. Zhao, Y. Liu, X. Li, H. Wang, Y. Zhang, H. Ma, Q. Wei, Label-free ECL immunosensor for the early diagnosis of rheumatoid arthritis based on asymmetric heterogeneous polyaniline-gold nanomaterial, Sens. Actuat. B: Chem. 257 (2018) 354–361.
[82] W. Kim, S.H. Lee, Y.J. Ahn, S.H. Lee, J. Ryu, S.K. Choi, S. Choi, A label-free cellulose SERS biosensor chip with improvement of nanoparticle-enhanced LSPR effects for early diagnosis of subarachnoid hemorrhage-induced complications, Biosens. Bioelectron. 111 (2018) 59–65.
[83] W. Gao, W. Wang, S. Yao, S. Wu, H. Zhang, J. Zhang, F. Jing, H. Mao, Q. Jin, H. Cong, Highly sensitive detection of multiple tumor markers for lung cancer using gold nanoparticle probes and microarrays, Anal. Chim. Acta 958 (2017) 77–84.
[84] Y. Fazaeli, O. Akhavan, R. Rahighi, M.R. Aboudzadeh, E. Karimi, H. Afarideh, In vivo SPECT imaging of tumors by 198,199 Au-labeled graphene oxide nanostructures, Mater. Sci. Eng. C 45 (2014) 196–204.
[85] A.D. Kurdekar, L.A. Chunduri, C.S. Manohar, M.K. Haleyurgirisetty, I.K. Hewlett, K. Venkataramaniah, Streptavidin-conjugated gold nanoclusters as ultrasensitive fluorescent sensors for early diagnosis of HIV infection, Sci. Adv. 4 (2018) eaar6280.
[86] G. Qiu, Z. Gai, Y. Tao, J. Schmitt, G.A. Kullak-Ublick, J. Wang, Dual-functional plasmonic photothermal biosensors for highly accurate severe acute respiratory syndrome coronavirus 2 detection, ACS Nano 14 (2020) 5268–5277.
[87] V.M. Corman, O. Landt, M. Kaiser, R. Molenkamp, A. Meijer, D.K. Chu, T. Bleicker, S. Brünink, J. Schneider, M.L. Schmidt, D.G. Mulders, B.L. Haagmans, B. van der Veer, S. van den Brink, L. Wijsman, G. Goderski, J.L. Romette, J. Ellis, M. Zambon, M. Peiris, H. Goossens, C. Reusken, M.P. Koopmans, C. Drosten, Detection of 2019 novel coronavirus (2019-nCoV) by real-time RT-PCR, Euro surveillance: bulletin Europeen sur les maladies transmissibles, Eur. Commun. Dis. Bull. 25 (2020).
[88] S. Ahmadi, N. Rabiee, M. Bagherzadeh, F. Elmi, Y. Fatahi, F. Farjadian, N. Baheiraei, B. Nasseri, M. Rabiee, N.T. Dastjerd, Stimulus-responsive sequential release systems for drug and gene delivery, Nano Today 34 (2020), 100914.
[89] C.M. Wolff, P.D. Frischmann, M. Schulze, B.J. Bohn, R. Wein, P. Livadas, M.T. Carlson, F. Jäckel, J. Feldmann, F. Würthner, All-in-one visible-light-driven water splitting by combining nanoparticulate and molecular co-catalysts on CdS nanorods, Nat. Energy 3 (2018) 862–869.
[90] L. Wang, W. Wang, Y. Chen, L. Yao, X. Zhao, H. Shi, M. Cao, Y. Liang, Heterogeneous p–n junction CdS/Cu2O nanorod arrays: synthesis and superior visible-light-driven photoelectrochemical performance for hydrogen evolution, ACS Appl. Mater. Interfaces 10 (2018) 11652–11662.
[91] K. Zhang, S. Lv, Z. Lin, M. Li, D. Tang, Bio-bar-code-based photoelectrochemical immunoassay for sensitive detection of prostate-specific antigen using rolling circle amplification and enzymatic biocatalytic precipitation, Biosens. Bioelectron. 101 (2018) 159–166.
[92] J. Fan, Y. Zang, J. Jiang, J. Lei, H. Xue, Beta-cyclodextrin-functionalized CdS nanorods as building modules for ultrasensitive photoelectrochemical bioassay of HIV DNA, Biosens. Bioelectron. 142 (2019), 111557.
[93] S.H. Qaddare, A. Salimi, Amplified fluorescent sensing of DNA using luminescent carbon dots and AuNPs/GO as a sensing platform: a novel coupling of FRET and DNA hybridization for homogeneous HIV-1 gene detection at femtomolar level, Biosens. Bioelectron. 89 (2017) 773–780.
[94] B. Babamiri, R. Hallaj, A. Salimi, Solid surface fluorescence immunosensor for ultrasensitive detection of hepatitis B virus surface antigen using PAMAM/CdTe@ CdS QDs nanoclusters, Fluoresc. Spectrosc. [Lect. Conf. "Methods Appl. Fluoresc. Spectrosc."] 6 (2018), 035013.
[95] K.-J. Huang, J. Li, Y.-M. Liu, X. Cao, S. Yu, M. Yu, Disposable immunoassay for hepatitis B surface antigen based on a graphene paste electrode functionalized with gold nanoparticles and a Nafion-cysteine conjugate, Mikrochim. Acta 177 (2012) 419–426.
[96] Y. Li, L. Tian, H. Jia, X. Pang, W. Cao, Q. Wei, An electrochemical immunosensor for ultrasensitive detection of HBsAg based on platinum nanoparticles loaded on natural montmorillonite, Anal. Methods 7 (2015) 9150–9157.
[97] K. Dashtian, S. Hajati, M. Ghaedi, L-phenylalanine-imprinted polydopamine-coated CdS/CdSe nn type II heterojunction as an ultrasensitive photoelectrochemical biosensor for the PKU monitoring, Biosens. Bioelectron. 165 (2020), 112346.
[98] A. Dumas, P. Couvreur, Palladium: a future key player in the nanomedical field? Chem. Sci. 6 (2015) 2153–2157.

[99] C. Zhang, D. Li, D. Li, K. Wen, X. Yang, Y. Zhu, Rolling circle amplification-mediated in situ synthesis of palladium nanoparticles for the ultrasensitive electrochemical detection of microRNA, Analyst 144 (2019) 3817–3825.
[100] L. Nie, M. Chen, X. Sun, P. Rong, N. Zheng, X. Chen, Palladium nanosheets as highly stable and effective contrast agents for in vivo photoacoustic molecular imaging, Nanoscale 6 (2014) 1271–1276.
[101] A. Rahi, N. Sattarahmady, H. Heli, An ultrasensitive electrochemical genosensor for Brucella based on palladium nanoparticles, Anal. Biochem. 510 (2016) 11–17.
[102] Q. Han, R. Wang, B. Xing, T. Zhang, M.S. Khan, D. Wu, Q. Wei, Label-free photoelectrochemical immunoassay for CEA detection based on CdS sensitized WO3@BiOI heterostructure nanocomposite, Biosens. Bioelectron. 99 (2018) 493–499.
[103] Y. Wu, G. Li, L. Zou, S. Lei, Q. Yu, B. Ye, Highly active DNAzyme-peptide hybrid structure coupled porous palladium for high-performance electrochemical aptasensing platform, Sens. Actuators B Chem. 259 (2018) 372–379.
[104] T. Yang, Y. Gao, Z. Liu, J. Xu, L. Lu, Y. Yu, Three-dimensional gold nanoparticles/prussian blue-poly(3,4-ethylenedioxythiophene) nanocomposite as novel redox matrix for label-free electrochemical immunoassay of carcinoembryonic antigen, Sens. Actuators B Chem. 239 (2017) 76–84.
[105] K. Barick, S. Singh, D. Bahadur, M.A. Lawande, D.P. Patkar, P. Hassan, Carboxyl decorated Fe3O4 nanoparticles for MRI diagnosis and localized hyperthermia, J. Colloid Interface Sci. 418 (2014) 120–125.
[106] S. Arsalani, E.J. Guidelli, M.A. Silveira, C.E. Salmon, J.F. Araujo, A.C. Bruno, O. Baffa, Magnetic Fe3O4 nanoparticles coated by natural rubber latex as MRI contrast agent, J. Magnet. Magnet. Mater. 475 (2019) 458–464.
[107] A.H. Rezayan, M. Mousavi, S. Kheirjou, G. Amoabediny, M.S. Ardestani, J. Mohammadnejad, Monodisperse magnetite (Fe3O4) nanoparticles modified with water soluble polymers for the diagnosis of breast cancer by MRI method, J. Magnet. Magnet. Mater. 420 (2016) 210–217.
[108] B. Wu, K. Deng, S.-T. Lu, C.-J. Zhang, Y.-W. Ao, H. Wang, H. Mei, C.-X. Wang, H. Xu, B. Hu, Reduction-active Fe3O4-loaded micelles with aggregation-enhanced MRI contrast for differential diagnosis of Neroglioma, Biomaterials 268 (2021), 120531.
[109] R. Nandi, S. Mishra, T.K. Maji, K. Manna, P. Kar, S. Banerjee, S. Dutta, S. Sharma, P. Lemmens, K.D. Saha, A novel nanohybrid for cancer theranostics: folate sensitized Fe 2 O 3 nanoparticles for colorectal cancer diagnosis and photodynamic therapy, J. Mater. Chem. B 5 (2017) 3927–3939.
[110] H. Hao, Q. Ma, F. He, P. Yao, Doxorubicin and Fe3O4 loaded albumin nanoparticles with folic acid modified dextran surface for tumor diagnosis and therapy, J. Mater. Chem. B 2 (2014) 7978–7987.
[111] S. Moradi, O. Akhavan, A. Tayyebi, R. Rahighi, M. Mohammadzadeh, H.S. Rad, Magnetite/dextran-functionalized graphene oxide nanosheets for in vivo positive contrast magnetic resonance imaging, RSC Adv. 5 (2015) 47529–47537.
[112] S. Felix, P. Kollu, B.P. Raghupathy, S.K. Jeong, A.N. Grace, Electrocatalytic oxidation of carbohydrates and dopamine in alkaline and neutral medium using CuO nanoplatelets, J. Electroanal. Chem. 739 (2015) 1–9.
[113] N. Torto, Recent progress in electrochemical oxidation of saccharides at gold and copper electrodes in alkaline solutions, Bioelectrochemistry 76 (2009) 195–200.
[114] F.C.U. Santos, L.L. Paim, J.L. da Silva, N.R. Stradiotto, Electrochemical determination of total reducing sugars from bioethanol production using glassy carbon electrode modified with graphene oxide containing copper nanoparticles, Fuel 163 (2016) 112–121.
[115] F. Cao, J. Gong, Nonenzymatic glucose sensor based on CuO microfibers composed of CuO nanoparticles, Anal. Chim. Acta 723 (2012) 39–44.
[116] J. Zhang, X. Zhu, H. Dong, X. Zhang, W. Wang, Z. Chen, In situ growth cupric oxide nanoparticles on carbon nanofibers for sensitive nonenzymatic sensing of glucose, Electrochim. Acta 105 (2013) 433–438.
[117] P.T. Garcia, A.A. Dias, J.A. Souza, W.K. Coltro, Batch injection analysis towards auxiliary diagnosis of periodontal diseases based on indirect amperometric detection of salivary α-amylase on a cupric oxide electrode, Anal. Chim. Acta 1041 (2018) 50–57.
[118] M. Kasiri, M. Rahaie, A visible and colorimetric nanobiosensor based on DNA-CuO nanoparticle for detection of single nucleotide polymorphism involved in sickle cell anemia disease, Mater. Today Commun. 27 (2021), 102423.
[119] J. Miao, C. Chen, J.Y. Lin, Humidity independent hydrogen sulfide sensing response achieved with monolayer film of CuO nanosheets, Sens. Actuat. B: Chem. 309 (2020), 127785.
[120] A. Tangerman, E. Winkel, Extra-oral halitosis: an overview, J. Breath Res. 4 (2010), 017003.
[121] K.F. Chung, Hydrogen sulfide as a potential biomarker of asthma, Expert Rev. Respir. Med. 8 (2014) 5–13.
[122] P. Wang, G. Zhang, T. Wondimu, B. Ross, R. Wang, Hydrogen Sulfide and Asthma, Wiley Online Library, 2011.
[123] Z. Yang, C. Yi, S. Lv, Y. Sheng, W. Wen, X. Zhang, S. Wang, Development of a lateral flow strip biosensor based on copper oxide nanoparticles for rapid and sensitive detection of HPV16 DNA, Sens. Actuat. B: Chem. 285 (2019) 326–332.
[124] M. Jannesari, O. Akhavan, H.R. Madaah Hosseini, B. Bakhshi, Graphene/CuO2 nanoshuttles with controllable release of oxygen nanobubbles promoting interruption of bacterial respiration, ACS Appl. Mater. Interfaces 12 (2020) 35813–35825.
[125] O. Akhavan, E. Ghaderi, Copper oxide nanoflakes as highly sensitive and fast response self-sterilizing biosensors, J. Mater. Chem. 21 (2011) 12935–12940.
[126] N.R. Shanmugam, S. Muthukumar, S. Prasad, A review on ZnO-based electrical biosensors for cardiac biomarker detection, Fut. Sci. OA 3 (2017) FSO196.
[127] Z.L. Wang, Nanostructures of zinc oxide, Mater. Today 7 (2004) 26–33.
[128] A. Janotti, C.G. Van de Walle, Fundamentals of zinc oxide as a semiconductor, Rep. Progr. Phys. 72 (2009), 126501.
[129] A.M. Faria, T. Mazon, Early diagnosis of Zika infection using a ZnO nanostructures-based rapid electrochemical biosensor, Talanta 203 (2019) 153–160.
[130] L.A. Chunduri, A. Kurdekar, B.E. Pradeep, M. Haleyurgirisetty, K. Venkataramaniah, I. Hewlett, Streptavidin conjugated ZnO nanoparticles for early detection of HIV infection, Adv. Mater. Lett. 8 (2017) 472–480.
[131] M. Salimi, S.M.R.M. Hosseini, Smartphone-based detection of lung cancer-related volatile organic compounds (VOCs) using rapid synthesized ZnO nanosheet, Sens. Actuators B 344 (2021), 130127.
[132] S.-C. Lee, H.-H. Park, S.-H. Kim, S.-H. Koh, S.-H. Han, M.-Y. Yoon, Ultrasensitive fluorescence detection of alzheimer's disease based on polyvalent directed peptide polymer coupled to a nanoporous ZnO nanoplatform, Anal. Chem. 91 (2019) 5573–5581.
[133] N. Akhtar, S.K. Metkar, A. Girigoswami, K. Girigoswami, ZnO nanoflower based sensitive nano-biosensor for amyloid detection, Mat. Sci. Eng.: C 78 (2017) 960–968.
[134] Z. Fei Yin, L. Wu, H. Gui Yang, Y. Hua Su, Recent progress in biomedical applications of titanium dioxide, Phys. Chem. Chem. Phys. 15 (2013) 4844–4858.
[135] J.Y. Lim, S.S. Lee, Sensitive detection of microRNA using QCM biosensors: sandwich hybridization and signal amplification by TiO2 nanoparticles, Anal. Methods 12 (2020) 5103–5109.
[136] X. Zhang, F. Wang, B. Liu, E.Y. Kelly, M.R. Servos, J. Liu, Adsorption of DNA oligonucleotides by titanium dioxide nanoparticles, Langmuir 30 (2014) 839–845.
[137] S. Sherin, S. Balachandran, A. Abraham, Curcumin incorporated titanium dioxide nanoparticles as MRI contrasting agent for early diagnosis of atherosclerosis-rat model, Vet. Anim. Sci. 10 (2020), 100090.
[138] W. Liu, L. Nie, F. Li, Z.P. Aguilar, H. Xu, Y. Xiong, F. Fu, H. Xu, Folic acid conjugated magnetic iron oxide nanoparticles for nondestructive separation and detection of ovarian cancer cells from whole blood, Biomater. Sci. 4 (2016) 159–166.
[139] K. Brince Paul, S. Kumar, S. Tripathy, S.R.K. Vanjari, V. Singh, S.G. Singh, A highly sensitive self assembled monolayer modified copper doped zinc oxide nanofiber interface for detection of Plasmodium falciparum histidine-rich protein-2: Targeted towards rapid, early diagnosis of malaria, Biosens. Bioelectron. 80 (2016) 39–46.
[140] N.J. Sajor, J.R. Foronda, R.S. Olarve, H.M. Dela Torre, M.G. Santos, T.B. Lopez, K.J. Haygood, G.N. Santos, V. Koledov, S.V. Gratowski, Synthesis of metal oxide nanomaterials for early lung disease detection, J. Phys. Conf. Ser. 1461 (2020), 012149.
[141] M. Asif, W. Haitao, D. Shuang, A. Aziz, G. Zhang, F. Xiao, H. Liu, Metal oxide intercalated layered double hydroxide nanosphere: With enhanced electrocatalyic activity towards H2O2 for biological applications, Sens. Actuators B 239 (2017) 243–252.
[142] W. Liang, Y. Zhuo, C. Xiong, Y. Zheng, Y. Chai, R. Yuan, A sensitive immunosensor via in situ enzymatically generating efficient quencher for electrochemiluminescence of iridium complexes doped SiO2 nanoparticles, Biosens. Bioelectron. 94 (2017) 568–574.
[143] X. Liu, L. Zhang, J. Wang, Design strategies for MOF-derived porous functional materials: Preserving surfaces and nurturing pores, J. Mater. 7 (2021) 440–459.

[144] S. Zhang, F. Rong, C. Guo, F. Duan, L. He, M. Wang, Z. Zhang, M. Kang, M. Du, Metal–organic frameworks (MOFs) based electrochemical biosensors for early cancer diagnosis in vitro, Coord. Chem. Rev. 439 (2021), 213948.
[145] Z.-H. Zhang, F.-H. Duan, J.-Y. Tian, J.-Y. He, L.-Y. Yang, H. Zhao, S. Zhang, C.-S. Liu, L.-H. He, M. Chen, D.-M. Chen, M. Du, Aptamer-embedded zirconium-based metal-organic framework composites prepared by de novo bio-inspired approach with enhanced biosensing for detecting trace analytes, ACS Sens. 2 (2017) 982–989.
[146] L. Du, W. Chen, J. Wang, W. Cai, S. Kong, C. Wu, Folic acid-functionalized zirconium metal-organic frameworks based electrochemical impedance biosensor for the cancer cell detection, Sens. Actuators B 301 (2019), 127073.
[147] J. Li, L. Liu, Y. Ai, Y. Liu, H. Sun, Q. Liang, Self-polymerized dopamine-decorated Au NPs and coordinated with Fe-MOF as a dual binding sites and dual signal-amplifying electrochemical aptasensor for the detection of CEA, ACS Appl. Mater. Interfaces 12 (2020) 5500–5510.
[148] J. Chang, X. Wang, J. Wang, H. Li, F. Li, Nucleic acid-functionalized metal-organic framework-based homogeneous electrochemical biosensor for simultaneous detection of multiple tumor biomarkers, Anal. Chem. 91 (2019) 3604–3610.
[149] X.J. Kong, X. Ji, T. He, L.H. Xie, Y.Z. Zhang, H. Lv, C. Ding, J.R. Li, A Green-emission metal-organic framework-based nanoprobe for imaging dual tumor biomarkers in living cells, ACS Appl. Mater. Interfaces 12 (2020) 35375–35384.
[150] G. Wang, Y. Fu, Z. Ren, J. Huang, S. Best, X. Li, G. Han, Upconversion nanocrystal 'armoured' silica fibres with superior photoluminescence for miRNA detection, Chem. Commun. 54 (2018) 6324–6327.
[151] X. Xia, Y. Hao, S. Hu, J. Wang, Hairpin DNA probe with 5′-TCC/CCC-3′ overhangs for the creation of silver nanoclusters and miRNA assay, Biosens. Bioelectron. 51 (2014) 36–39.
[152] S.-K. Sun, H.-F. Wang, X.-P. Yan, Engineering persistent luminescence nanoparticles for biological applications: from biosensing/bioimaging to theranostics, Acc. Chem. Res. 51 (2018) 1131–1143.
[153] Y. Lv, D. Ding, Y. Zhuang, Y. Feng, J. Shi, H. Zhang, T.-L. Zhou, H. Chen, R.-J. Xie, Chromium-doped zinc gallogermanate@ zeolitic imidazolate framework-8: a multifunctional nanoplatform for rechargeable in vivo persistent luminescence imaging and pH-responsive drug release, ACS Appl. Mater. Interfaces 11 (2018) 1907–1916.
[154] Z. Gao, Y. Li, X. Zhang, J. Feng, L. Kong, P. Wang, Z. Chen, Y. Dong, Q. Wei, Ultrasensitive electrochemical immunosensor for quantitative detection of HBeAg using Au@ Pd/MoS2@ MWCNTs nanocomposite as enzyme-mimetic labels, Biosens. Bioelectron. 102 (2018) 189–195.
[155] F. Li, Y. Li, J. Feng, Y. Dong, P. Wang, L. Chen, Z. Chen, H. Liu, Q. Wei, Ultrasensitive amperometric immunosensor for PSA detection based on Cu2O@ CeO2-Au nanocomposites as integrated triple signal amplification strategy, Biosens. Bioelectron. 87 (2017) 630–637.
[156] A.A. Saeed, J.L.A. Sánchez, C.K. O'Sullivan, M.N. Abbas, DNA biosensors based on gold nanoparticles-modified graphene oxide for the detection of breast cancer biomarkers for early diagnosis, Bioelectrochemistry 118 (2017) 91–99.
[157] A. Sabahi, R. Salahandish, A. Ghaffarinejad, E. Omidinia, Electrochemical nano-genosensor for highly sensitive detection of miR-21 biomarker based on SWCNT-grafted dendritic Au nanostructure for early detection of prostate cancer, Talanta 209 (2020), 120595.
[158] Y. Yang, Q. Yan, Q. Liu, Y. Li, H. Liu, P. Wang, L. Chen, D. Zhang, Y. Li, Y. Dong, An ultrasensitive sandwich-type electrochemical immunosensor based on the signal amplification strategy of echinoidea-shaped Au@ Ag-Cu2O nanoparticles for prostate specific antigen detection, Biosens. Bioelectron. 99 (2018) 450–457.
[159] C. Pothipor, N. Wiriyakun, T. Putnin, A. Ngamaroonchote, J. Jakmunee, K. Ounnunkad, R. Laocharoensuk, N. Aroonyadet, Highly sensitive biosensor based on graphene–poly (3-aminobenzoic acid) modified electrodes and porous-hollowed-silver-gold nanoparticle labelling for prostate cancer detection, Sens. Actuators B 296 (2019), 126657.
[160] G. Choi, E. Kim, E. Park, J.H. Lee, A cost-effective chemiluminescent biosensor capable of early diagnosing cancer using a combination of magnetic beads and platinum nanoparticles, Talanta 162 (2017) 38–45.
[161] M. Dadmehr, M. Hosseini, S. Hosseinkhani, M. Ganjali, M. Khoobi, H. Behzadi, M. Hamedani, R. Sheikhnejad, DNA methylation detection by a novel fluorimetric nanobiosensor for early cancer diagnosis, Biosens. Bioelectron. 60 (2014) 35–44.
[162] L. Zhao, J. Blackburn, C.L. Brosseau, Quantitative detection of uric acid by electrochemical-surface enhanced Raman spectroscopy using a multilayered Au/Ag substrate, Anal. Chem. 87 (2015) 441–447.
[163] A. Afzalinia, M. Mirzaee, Ultrasensitive fluorescent miRNA biosensor based on a "sandwich" oligonucleotide hybridization and fluorescence resonance energy transfer process using an Ln (III)-MOF and Ag nanoparticles for early cancer diagnosis: application of central composite design, ACS Appl. Mater. Interfaces 12 (2020) 16076–16087.
[164] M. Šimšíková, J. Čechal, A. Zorkovská, M. Antalík, T. Šikola, Preparation of CuO/ZnO nanocomposite and its application as a cysteine/homocysteine colorimetric and fluorescence detector, Colloids Surf. B 123 (2014) 951–958.
[165] M. Haque, H. Fouad, H.-K. Seo, A.Y. Othman, A. Kulkarni, Z.A. Ansari, Investigation of Mn doped ZnO nanoparticles towards ascertaining myocardial infarction through an electrochemical detection of myoglobin, IEEE Access 8 (2020) 164678–164692.
[166] W. Kong, F. Qu, L. Lu, A photoelectrochemical aptasensor based on pn heterojunction CdS-Cu 2 O nanorod arrays with enhanced photocurrent for the detection of prostate-specific antigen, Anal. Bioanal. Chem. 412 (2020) 841–848.
[167] N.A.S. Omar, Y.W. Fen, J. Abdullah, M.H.M. Zaid, M.A. Mahdi, Structural, optical and sensing properties of CdS-NH2GO thin film as a dengue virus E-protein sensing material, Optik 171 (2018) 934–940.
[168] J. Wang, X. Wang, H. Tang, Z. Gao, S. He, J. Li, S. Han, Ultrasensitive electrochemical detection of tumor cells based on multiple layer CdS quantum dots-functionalized polystyrene microspheres and graphene oxide–polyaniline composite, Biosens. Bioelectron. 100 (2018) 1–7.
[169] G.-C. Fan, X.-L. Ren, C. Zhu, J.-R. Zhang, J.-J. Zhu, A new signal amplification strategy of photoelectrochemical immunoassay for highly sensitive interleukin-6 detection based on TiO2/CdS/CdSe dual co-sensitized structure, Biosens. Bioelectron. 59 (2014) 45–53.
[170] M. Ehsani, M.J. Chaichi, S.N. Hosseini, Comparison of CuO nanoparticle and CuO/MWCNT nanocomposite for amplification of chemiluminescence immunoassay for detection of the hepatitis B surface antigen in biological samples, Sens. Actuators B 247 (2017) 319–328.
[171] L. Ruiyi, P. Tinling, C. Hongxia, S. Jinsong, L. Zaijun, Electrochemical detection of cancer cells in human blood using folic acid and glutamic acid-functionalized graphene quantum dot-palladium@gold as redox probe with excellent electrocatalytic activity and target recognition, Sens. Actuators B 309 (2020), 127709.
[172] J.-j. Li, L. Shang, L.-P. Jia, R.-N. Ma, W. Zhang, W.-L. Jia, H.-S. Wang, K.-H. Xu, An ultrasensitive electrochemiluminescence sensor for the detection of HULC based on Au@ Ag/GQDs as a signal indicator, J. Electroanal. Chem. 824 (2018) 114–120.
[173] Y. He, S. Chen, L. Huang, Z. Wang, Y. Wu, F. Fu, Combination of magnetic-beads-based multiple metal nanoparticles labeling with hybridization chain reaction amplification for simultaneous detection of multiple cancer cells with inductively coupled plasma mass spectrometry, Anal. Chem. 91 (2018) 1171–1177.
[174] P. Srinivasan, D. Prakalya, B. Jeyaprakash, UV-activated ZnO/CdO nn isotype heterostructure as breath sensor, J. Alloys Compd. 819 (2020), 152985.
[175] J. Ma, S.M.-Y. Lee, C. Yi, C.-W. Li, Controllable synthesis of functional nanoparticles by microfluidic platforms for biomedical applications – a review, Lab Chip 17 (2017) 209–226.
[176] S. Majumder, M.J. Deen, Smartphone sensors for health monitoring and diagnosis, Sensors (Basel) 19 (2019) 2164.
[177] Z. Liao, Y. Zhang, Y. Li, Y. Miao, S. Gao, F. Lin, Y. Deng, L. Geng, Microfluidic chip coupled with optical biosensors for simultaneous detection of multiple analytes: a review, Biosens. Bioelectron. 126 (2019) 697–706.
[178] N. Rabiee, S. Ahmadi, Y. Fatahi, M. Rabiee, M. Bagherzadeh, R. Dinarvand, B. Bagheri, P. Zarrintaj, M.R. Saeb, T.J. Webster, Nanotechnology-assisted microfluidic systems: from bench to bedside, Nanomedicine 16 (2021) 237–258.
[179] N. Convery, N. Gadegaard, 30 years of microfluidics, Micro Nano Eng. 2 (2019) 76–91.
[180] L. Guo, Y. Shi, X. Liu, Z. Han, Z. Zhao, Y. Chen, W. Xie, X. Li, Enhanced fluorescence detection of proteins using ZnO nanowires integrated inside microfluidic chips, Biosens. Bioelectron. 99 (2018) 368–374.
[181] M.S. Draz, A. Vasan, A. Muthupandian, M.K. Kanakasabapathy, P. Thirumalaraju, A. Sreeram, S. Krishnakumar, V. Yogesh, W. Lin, X.G. Yu, R.T. Chung, H. Shafiee, Virus detection using nanoparticles and deep neural network–enabled smartphone system, Sci. Adv. 6 (2020) eabd5354.

[182] A. Roda, E. Michelini, M. Zangheri, M. Di Fusco, D. Calabria, P. Simoni, Smartphone-based biosensors: a critical review and perspectives, TrAC Trends Anal. Chem. 79 (2016) 317–325.
[183] M.R. Younis, C. Wang, M.A. Younis, X.-H. Xia.
[184] X. Huang, D. Xu, J. Chen, J. Liu, Y. Li, J. Song, X. Ma, J. Guo, Smartphone-based analytical biosensors, Analyst 143 (2018) 5339–5351.
[185] W.I. Lee, Y. Park, J. Park, S. Shrivastava, Y.M. Son, H.J. Choi, J. Lee, B. Jeon, H. Lee, N.E. Lee, A smartphone fluorescence imaging-based mobile biosensing system integrated with a passive fluidic control cartridge for minimal user intervention and high accuracy, Lab Chip 19 (2019) 1502–1511.
[186] Y.-P. Hsu, N.-S. Li, Y.-T. Chen, H.-H. Pang, K.-C. Wei, H.-W. Yang, A serological point-of-care test for Zika virus detection and infection surveillance using an enzyme-free vial immunosensor with a smartphone, Biosens. Bioelectron. 151 (2020), 111960.
[187] Y. Xia, Y. Chen, Y. Tang, G. Cheng, X. Yu, H. He, G. Cao, H. Lu, Z. Liu, S.Y. Zheng, Smartphone-based point-of-care microfluidic platform fabricated with a ZnO nanorod template for colorimetric virus detection, ACS Sens. 4 (2019) 3298–3307.
[188] I. Khan, K. Saeed, I. Khan, Nanoparticles: properties, applications and toxicities, Arabian J. Chem. 12 (2019) 908–931.
[189] J.R. Choi, Development of point-of-care biosensors for COVID-19, Front. Chem. 8 (2020) 517.